Escola d'Enginyeria de Telecomunicació i Aeroespacial de Castelldefels

UNIVERSITAT POLITÈCNICA DE CATALUNYA

FINAL DEGREE PROJECT

TITLE:	**Numerical simulation and validation of ultrasonic de-icing system**
FIELD OF STUDY:	**Degree of Aeronavigation & Airports engineering**
AUTHORS:	**Alexis Chica Gil** **Borja Tarré Gómez**
SUPERVISOR:	**Mr. Xu Yuangming**
DATA:	**26 January 2018**

ABSTRACT

This work presents the analytic and experimental research of de-icing method with piezoelectric transducer as actuators.

For the reason of flight conditions like altitude, high and humidity. To meet the requirements for flight, deicing measures must be taken in consideration.

There are lots of existing deicing methods, but the main problem is that the loss of power with them is very big increasing the consumption of fuel and decreasing the efficiency of the flight. With the development of piezoelectric ceramic technology, shear vibration deicing is more concerned for their low power consumption. Shear stress between surface and ice is generated by the forced vibration which is driven by piezoelectric.

The device achieves the deicing purpose activating resonant frequencies of a structure using piezoelectric ceramic actuators to generate enough shear stress at the interface, between the surface and ice, to break the adhesion stress between them.

In this study, we study the effect of shear stress generated for different distances between ceramic piezoelectric, and then analyze the relations of the shear stress and frequency.

First, a numerical method was validated to assist the design of such systems. Numerical simulations were performed for the case of a flat plate testing the natural modes and harmonic response by the software ANSYS, which proves the feasibility to remove ice by piezoelectric ceramic actuator in theory.

And then, validated experimentally. The model was then used to study important design parameters such as actuator positioning and the distance between them.

.

Keywords: piezoelectric, de-icing, shear stress, PZT

本文介紹了一種以壓電換能器作為執行器的除冰方法的分析和實驗研究。

由於飛行條件，如海拔高度和濕度的原因。為了達到飛行要求，必須採取除冰措施。

有很多現有的除冰方法，但是與他們的功率損失是非常大的。隨著壓電陶瓷技術的發展，
剪切振動除冰技術更加關注低功耗。表面和冰之間的剪切應力是由壓電驅動的受迫振動產生的。

該裝置實現了利用壓電陶瓷致動器激活結構的共振頻率的除冰目的，以在表面和冰之間的界面處產生足夠的剪切應力以打破它們之間的粘附應力。

在本研究中，我們研究了不同長度的陶瓷壓電材料產生的剪切應力的影響，然後分析了剪切應力與頻率的關係。

首先，數值方法被驗證來輔助這種系統的設計。對ANSYS平台測試自然模態和諧波響應的平板情況進行了數值模擬，從理論上證明了利用壓電陶瓷驅動器去除冰塊的可行性。

然後通過實驗驗證。然後使用該模型來研究重要的設計參數，例如執行器定位和它們之間的距離。
。

關鍵詞：壓電，除冰，剪應力，PZT

INDEX

TABLES

FIGURE TABLE

II Introduction

The study of this project will analyze the viability of the ultrasonic de-icing system focusing on the piezoelectric ceramic transducer PZT-4.

II.1 Project Objectives

The purpose of the project has as main target find an alternative de-icing device better than the used nowadays, that consume big amounts of energy and heat. Through the physics of ultrasonic, by piezoelectric materials used in transducers.

By the transducers PZT-4, a series of researches and simulations by software has been done to determine which configuration of this PZT suits better the de-icing effect.

II.2 Scope of the project

This project is limited to study and analyze how the distance between the transducers suits better on a surface to reach the maximum de-icing effect.

To be more accurate, the field of the study is to analyze how the distance between two transducers in a flat surface affects the total stress generated by the piezoelectric materials and which is the optimal position between the transducers to maximize the de-icing effect.

This work does not include another several parameters or factors that can also affect the de-icing effect like, different temperatures, different depth of ice, more than two transducers, another types of piezoelectric materials, material of the laminar plate...

III Aircraft icing

III.1 Issues

Nowadays aircraft icing, in particular in-flight icing, poses serious threat to flight safety. This occurs when the air contains droplets of supercooled liquid water.

Icing conditions are characterized quantitatively by the average droplet size, the liquid water content and the air temperature. These parameters affect the extent and speed that characterize the formation of ice on an aircraft.
Federal Aviation Regulations contain a definition of icing conditions that some aircraft are certified to fly into. So-called SLD, or supercooled large droplet, conditions are those that exceed that specification and represent a particular hazard to aircraft.

Figure 1. Ice droplets

In-flight aircraft icing has been considered as a dangerous phenomenon posing significant risk to the safety of the flight.

Many researchers have indicated that ice accreted on these spots, in particular, on lifting surface, leads to aerodynamic configuration degradation.
Icing reduces aircraft efficiency by increasing weight, reducing lift, decreasing thrust, and increasing drag. With the accumulation of ice, the wing surface roughness increases, which not only results in airfoil distortion, but also induces boundary layer transition. Both friction drag and pressure drag increase substantially due to icing. When in-flight icing leads to an increase in drag,

aircraft engine requires providing extra thrust to overcome resistance, which necessitates additional fuel consumption.

Specific fuel consumption is an important economic index which serious concern in aircraft design; therefore, increase in fuel consumption becomes a crucial problem that cannot be neglected.

Besides, wing icing promotes boundary layer separation, thus decreasing lift and critical angle of attack. Still worse, icing on the horizontal tail seriously damages the stability and manipulation of airplanes and a partial or complete blockage of the air inlet to any part of a pitot static system can be produced inducing to errors in the readings of pressure instruments such as Altimeters, Airspeed indicators, and Vertical Speed Indicators. Severe ice accretions may lead to disastrous fatal accidents.

III.2 Current Solutions

To reduce the potential harmful effects of aircraft icing, a number of anti/de-icing systems have been developed. Thus, anti/de-icing techniques are researched extensively in Aeronautical Engineering and in Wind Energy Engineering field. Wind energy is a significant renewable and sustainable type of resource. However, accumulation of ice on wind turbines that work under harsh weather conditions, leads to deformation of blades which may cause increase of torque as well as crease of efficiency and power output.

Figure 2. Ice wing forms

Aircraft and engine ice protection systems are generally of two designs: either they remove ice after has formed, or they prevent it from forming. The first type of system is referred to as a de-icing system and the second one as anti-icing system, and both types could use passive or active methods. Passive methods take advantage of the physical properties of surface to eliminate ice or prevent the formation of ice, while active methods use external systems and require energy power supply that is either thermal, chemical or ultrasonic method.

Although, no passive or active anti-icing and de-icing systems are totally effective to prevent initial and subsequent icing, during icing events some systems have been proved to maintain power output, minimize dynamic impact of icing and, perhaps most importantly, avoid ice hazard close to habitable sites.

Figure 3. Passive de-icing system

Consequently, due to most anti-icing and de-icing systems are based on heating, wind turbines need more power to operate. The extra power will be added to the consumption of the nacelle cold climate package. Furthermore, additional maintenance should be planned.

In the following points, some of the most common anti-icing and de-icing systems will be shown.

III.2.1 De-icing

Deicing equipment is designed to remove ice after it begins to accumulate on the airframe.

A de-icing system has two very attractive attributes. First, it can utilize a variety of means to transfer the energy used to remove the ice. This allows the consideration of mechanical (principally pneumatic), electrical and thermal methods. The second attribute is that it is energy efficient, requiring energy only periodically when ice is being removed, with some mechanical designs requiring relatively little energy overall. This is a significant consideration when designing ice protection for aircraft with limited excess power.

The principal drawback to the de-icing system is that, by default, the aircraft will operate with ice accretions for the majority of the time in icing conditions. The only time it will be free of ice accretions will be the time during and immediately after the cycling of the de-ice system. This requires an understanding on the part of the designer and the pilot of what effects the ice accretions will have on aircraft performance, both prior to and during system operation.

Any design which utilizes either a mechanical means of breaking the bond of ice to the surface, or which operates on a periodic cycle, is necessarily a de-ice system.

III.2.1.1 Electro-Thermal Deicing Systems

Conventional electro-thermal deicing systems use a resistive heater that is attached to the part of the leading edge to be protected, with particular emphasis on the limits of ice impingement, the so-called impingement zone. The heater applied to the airfoil is conventionally segmented into several sections. Each section consists of several individual heaters (typically 5) with a narrow side in the chord wise direction, and the long side along the span wise direction.

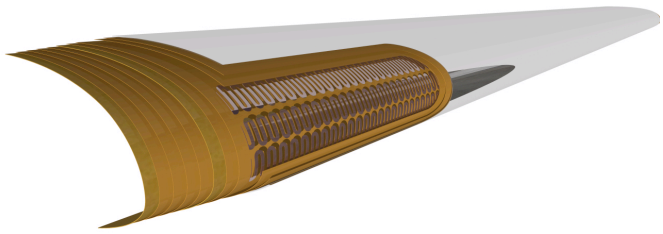

Figure 4. Airfoil segmented heaters

III.2.1.2 Pneumatic De-Ice Boots

A very common active de-icing system utilizes pneumatically inflated rubber boots on the leading edges of airfoil surfaces. This typically includes the wings and horizontal stabilizer, but may also include struts, cargo pods, or even antennae. The system uses relatively low pressure air to rapidly inflate and deflate the boot. This is usually done in a sequence of segments, for example, the outer wings followed by the inner wings followed by the horizontal stabilizer. Depending on the manufacturer's specifications, the system may be operated either automatically, through a timing circuit, or manually, using a cockpit control to initiate the boot cycle sequence.

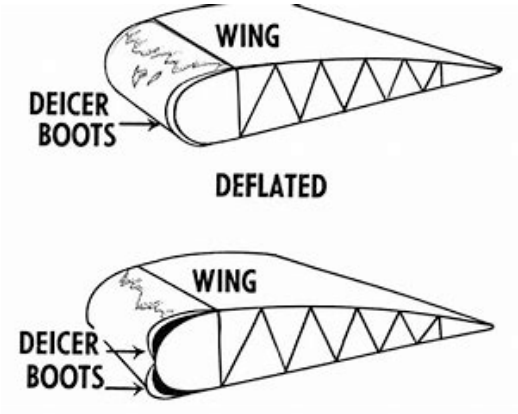

Figure 5. Pneumatic boot designs

Early pneumatic boot designs had relatively low volume air supplies to draw from, and were slower to inflate and deflate. A phenomenon which was thought to be occasionally observed with these systems was known as "ice bridging", in which the boot expanded under the ice and stretched it without breaking its structure. This led to a space beneath the ice shape which allowed the boot to inflate and deflate with no effect. The problem was addressed by allowing a particular thickness of ice to develop before inflating the boot. Once the requisite thickness was attained, the boot inflation would shatter the ice and clear it off the surface.

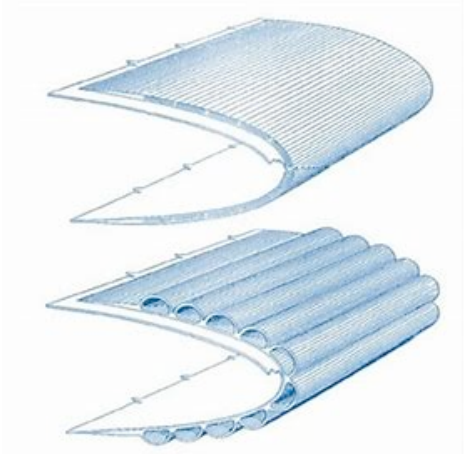

Figure 6. De-icer boots

III.2.2 Anti-icing

Anti-icing systems reverse this paradigm. Properly used, they prevent the formation of ice continuously, resulting in a clean wing with no aerodynamic penalties. An anti-icing system must have a means of continuously delivering energy or chemical flow to a surface in order to prevent the bonding of ice. The typical thermal anti-icing system does this at significant energy expense. The concept is not viable for aircraft that do not have the requisite excess energy available during all flight phases. An exception to this is the use of a chemical system such as TKS.

III.2.2.1 Thermal Systems

A thermal anti-ice system is designed to operate in one of two ways: fully evaporative or running wet. In the former case, sufficient energy is provided to cause impinging supercooled water to completely evaporate. This has an obvious advantage of protecting the aft, unheated portion of the airfoil, since the evaporated water cannot re-condense before the airfoil has passed. It is a very effective means of ice protection, but the concept requires a great deal of excess energy.

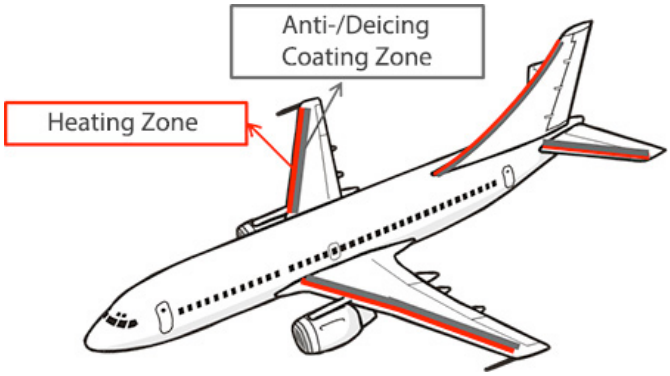

Figure 7. Thermal anti-icing system

A running wet system can only prevent impinging water from freezing. This requires rather less energy. However, it can fail to prevent runback ice, which forms when the running water passes aft of the heated surface and freezes.

Any fully evaporative system will necessarily transition through a running wet phase as it both heats and cools. The ideal method for operating a fully evaporative system is to activate it prior to entering icing conditions, thus allowing the surface to stabilize at the required temperature.

A thermal de-icing system requires much less energy. Using either engine bleed air, exhaust-heated air, or electrical heating, this system is intended only to periodically break the bond between accreted ice and the surface.

III.2.2.2 Chemical System

The TKS (Tecalemit-Kilfrost-Sheepbridge Stokes) Ice Protection System, is a fluid-based ice protection system used to help aircraft safely exit in-flight icing conditions. The system uses a glycol-based fluid to cover the critical surfaces of an aircraft and prevent the risk of any ice forming on the leading edges of the wings. The system can also break the ice that has accumulated (chemically).

Ice Protection with the TKS Ice Protection system is achieved by mounting laser-drilled titanium porous panels on the leading edges of the airframe. The panel skin is perforated with eight hundred 0.0025-inch-diameter laser-drilled holes per square inch. TKS fluid exudes through the panels on the leading edges of the wings, horizontal stabilizers. Fluid is also thoroughly distributed from the slinger-ring on the propeller and from the windshield spraybar.

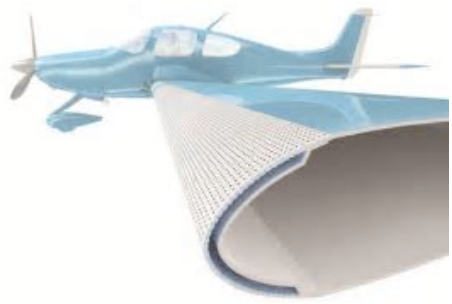

Figure 8. TKS Titanium porous panels

III.2.2.3 Bleed air system

A bleed air system is the method used by most larger jet aircraft to keep flight surfaces above the freezing temperature required for ice to accumulate. The hot air is "bled" off the jet engine into piccolo tubes routed through wings, tail surfaces, and engine inlets. The spent bleed air is exhausted through holes in the lower surface of the wing.

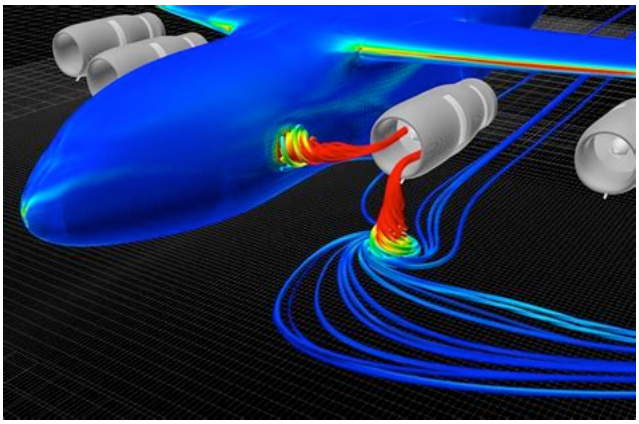

Figure 9. Bleed air system

III.3 Proposed Alternative Ultrasonic Deicing

Compared to other methods, and specially the thermal ones, ultrasonic guided wave (UGW) de-icing method consumes less energy and produces less weight increase. Therefore, comparatively, this technology exhibits significant development prospects in improving energy efficiency.

Ultrasonic anti/de-icing technique was first proposed by prof. Jose L. Palacios in 2004. In his research the use of ultrasonic shear and lamb waves for composite rotor de-icing were investigated. Such technique is based on the fact that the adhesive bond of ice-substrate interface is relatively weak in shear strength compared with the interface forces within composite blades. When high-energy ultrasonic waves travel through a plate-ice layered system, the shear stresses at contact surface or interface between the plate and ice layer, is caused by the difference of wave propagation speed produced due to difference of physical properties existed in ice and the plate.
Such shear stresses can not only debond the ice layer but also break the ice layer. The piezoelectric actuators can be used to produce local shears at the locations of ice accretion to weaken the interface and subsequently de-ice the surface with normal impulse forces.

Figure 10. Ice block

How the parameters of the piezoelectric actuator and the transducer affect the de-icing are important topics for future studies. This research, as it is said before, will focus in how the distance between two transducers will affect the de-icing and which case will be worth it for de-icing. Once the best case has been found, the next step will be trying to figure out how the thickness of the ice affects the system.

IV Transducer Device

The piezoelectric transducers are devices that work on the principle of piezoelectric effect. When mechanical stress or forces are applied to some materials along certain planes, they produce electric voltage. For our field of research, it is used that principle but in an inverse way, generating force or shear to a ceramic piezometer applying electricity.

The active element is the heart of the transducer, as it converts the electrical energy to acoustic energy, and vice versa. The active element is basically a piece of polarized material with electrodes attached to two of its opposite faces.

When an electric field is applied across the material, the polarized molecules will align themselves with the electric field, resulting in induced dipoles within the molecular or crystal structure of the material. This alignment of molecules will cause the material to change dimensions. This phenomenon is known as electrostriction. In addition, a permanently-polarized material will produce an electric field when the material changes dimensions as a result of an imposed mechanical force. This phenomenon is known as the piezoelectric effect.

Figure 11. Transducer device

The finite element method (FEM) is used to get the relationships between the length and thickness of piezoelectric ceramic transducer (PZT) and the vibration intensity of the modes being excited. The thickness of PZT should be thin as long as the strength requirements are met. The maximum shear stress on the bond layer concentrates on the edge of length direction, and the amplitude depends upon the strain on the surface of plate under the edge of ice.

The active element of most acoustic transducers used today is a ceramic piezoelectric, which can be cut in various ways to produce different wave modes.
They also operate at low voltage and are usable up to about 300^{o}C.

V The principle of ultrasonic de-icing

As it is explained in the paper of Congbo Yin, Zhengong Zhang Zhenjun Wang and Hui Guo named “Numerical simulation and experimental validation of ultrasonic de-icing system for wind turbine blade” published by Elsevier (2016); “under the action of ultrasonic actuators [4], there are two kinds of waves propagate in the composite plate-ice layered system-lamb wave and SH wave, which can cause interface shear stress between ice and substrate. The composite plates-ice layered system is shown in the following figure.

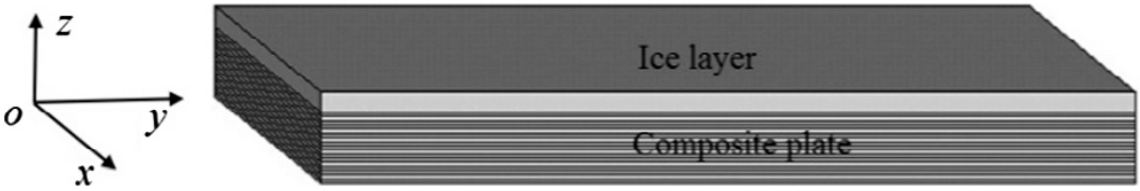

Figure 12. The schematic of the anisotropic multi-layer structure.

The wave functions of lamb wave and SH wave can be written as:

$$\frac{\partial^2 u_i}{\partial t^2} = c_{ijkl}\frac{\partial^2 u_i}{\partial x_j \partial x_k} \quad [1]$$

In equation [1]; q, c, u_i are the density, stiffness matrix and displacement field of the media respectively. Here, the elastic constant matrix (stiffness matrix) used in the calculation is listed in equation [2]:

In equation [1]; q, c, u_i are the density, stiffness matrix and displacement field of the media respectively. Here, the elastic constant matrix (stiffness matrix) used in the calculation is listed in equation [2]:

$$c = \begin{pmatrix} c_{11} & c_{12} & c_{13} & 0 & 0 & 0 \\ c_{12} & c_{11} & c_{13} & 0 & 0 & 0 \\ c_{13} & c_{13} & c_{33} & 0 & 0 & 0 \\ 0 & 0 & 0 & c_{44} & 0 & 0 \\ 0 & 0 & 0 & 0 & c_{55} & 0 \\ 0 & 0 & 0 & 0 & 0 & c_{66} \end{pmatrix} \quad [2]$$

Assume the displacement can be written as:

$$u_i = A_i e^{ik(x_1 + px_3 - ct)} \quad [3]$$

By solving equation [3] can obtain the solutions of SH wave and Lamb wave propagating in anisotropic elastic media. In equation [3]), u_i is the polarization vector representing the displacement vector in each direction, k is the wave number along x_1 direction, c is the phase velocity along x1direction, and p is the ratio of the wave number in the x_3 direction with respect to the wave number in the x_1 direction.

The guided waves are assumed to be propagating along the x_1-x_3 plane and the displacement is independent of the x_2 direction. Substitute the formal solution into the governing equation to obtain the Christoffel's equation, which is shown in equation [4].

$$\begin{bmatrix} \lambda_{11} - pc^2 & \lambda_{12} & \lambda_{13} \\ \lambda_{12} & \lambda_{22} - pc^2 & \lambda_{23} \\ \lambda_{13} & \lambda_{23} & \lambda_{33} - pc^2 \end{bmatrix} \begin{bmatrix} U_1 \\ U_2 \\ U_3 \end{bmatrix} = 0 \quad [4]$$

Here, the values of k_{im} (i, m = 1, 2, 3) can be obtained from equation [5]:

$$\lambda_{im} = C_{iklm} n_k n_l \quad [5]$$

Where n_k, n_l are the direction cosines of the normal to the wave front. Our purpose is to get a nontrivial solution for equation [4]. The final solutions of the ultrasonic guided waves in the layered structure are the linear combinations of the partial wave solutions. Assume that the displacement and stress are expressed in the following equations with undetermined coefficients A_k.

$$u_1 = \sum_{k=1}^{4} A_k e^{ik(x_1 + p_k x_3 - ct)} \quad [6]$$

$$u_2 = \sum_{k=1}^{2} A_k e^{ik(x_1 + p_k x_3 - ct)} \quad [7]$$

$$u_3 = \sum_{k=1}^{4} A_k U_{3k} e^{ik(x_1 + p_k x_3 - ct)} \quad [8]$$

$$\tau_{13} = \sum_{k=1}^{4} A_k [p_k + U_{3k}] e^{ik(x_1 + p_k x_3 - ct)} \quad [9]$$

$$\tau_{23} = \sum_{k=1}^{2} A_k p_k \mu (ik) e^{ik(x_1 + p_k x_3 - ct)} \quad [10]$$

$$\tau_{33} = \sum_{k=1}^{4} A_k [\lambda + (\lambda + 2\mu) p_k U_{3k}] (ik) e^{ik(x_1 + p_k x_3 - ct)} \quad [11]$$

Where A_k are the weighting coefficients of the partial waves. In order to solve for the weighting coefficient vector A_k, boundary conditions are applied according to the above equations.

For lamb waves on a 2 layered system, 8 boundary conditions are identified: free shear and longitudinal stress at the top surface (2 boundary conditions), free shear and longitudinal stress at the bottom surface (2 boundary conditions), continuity in u_1 and u_3 displacement at the interface (2 boundary conditions), continuity in the interface shear and longitudinal stresses (2 boundary conditions).

For lamb waves, an 8x8 matrix is formed by the eight equations derived by the system's boundary conditions.

For shear waves on a 2 layered system, 4 boundary conditions are identified: Free shear stress at the top surface (1 boundary conditions). Free shear stress at the bottom surface (1 boundary conditions). Continuity in u2, displacement at the interface (1 boundary conditions).

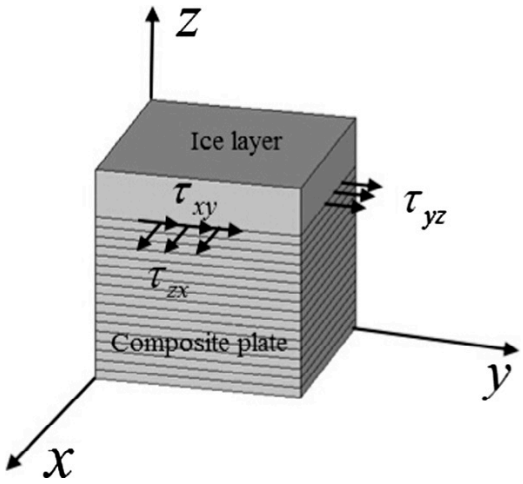

Figure 13: The shear stresses at a contact surface between composite plate and ice cover.

Under the action of ultrasonic actuators, the finite element vibration equation of the structure of ultrasonic actuators, composite plate and ice layer is shown in formula [12]:

$$F = ([K_{nn}] - \omega^2[M] - j\omega[R])U + [K_{n\Phi}]\Phi\left(\frac{I}{j\omega}\right) = [K_{\Phi n}]U + [K_{\Phi\Phi}]\Phi \quad [12]$$

Where F is the applied mechanical stress, I is excitation current, U is plastic displacement field, U is the electric potential strength, [K_{nn}] is the elastic rigidity matrix, [K_{nU}] is the piezoelectric rigidity matrix, [K_{UU}] is the permittivity matrix, [M] is the mass matrix, [R] is the dissipative matrix, x is the angular frequency. The finite element matrix equation of harmonic analysis can be written as formula [13]:

$$\begin{bmatrix} K_{nn} - \omega^2 M & K_{n\Phi} \\ K_{n\Phi} & K_{\Phi\Phi} \end{bmatrix} \begin{bmatrix} U \\ \Phi \end{bmatrix} = \begin{bmatrix} 0 \\ -Q \end{bmatrix} \quad [13]$$

The shear stresses at contact surface between composite plate and ice layer are shown in figure 2. Among these three stresses, the role of s_{zx} and s_{zy} is to get rid of the ice, while s_{xy} is to break the ice. If the resultant force of those three stresses is greater than the largest ice adhesion stress, the ice will be removed from the composite plate-ice layered system.

In order to avoid frequency dispersion, the installation distance between piezoelectric wafers should meet the requirement of formula [14]:

$$d = \left(n + \frac{1}{2}\right)\lambda_f, \qquad n = 1,2,3,4 \ldots \quad [14]$$

V.1 Measurement of ice adhesion strength

The calculus or the prediction of the ice adhesion in a substrate plate is not well known and not easy to calculate.

This value of ice adhesion is really dependent on the roughness of the material surface, temperature and many other influencing factors.

For this reason, this value was taken as reference in the study done by Mr Wang and Mr Xu, "*An effect assessment and prediction method of ultrasonic de-icing for composite wind turbine blades*". They carried out the study where they conclude that the average value of ice adhesion in a composite substrate rounds the value of 0.4MPa.

VI Simulations

VI.1 The parameters of the simulation

VI.1.1 Software

In order to verify the feasibility of the ultrasonic de-icing system, it is done an experiment based on software simulations with ANSYS. Creating the most similar environment as in real life.

Figure 14. ANSYS logo

Once we have all the project developed on ANSYS, we can modify a lot of parameters that affect the system but, for the purpose of this research only it is going to be set and modified the distance between the two transducers.
The main objective is to find a solution with a standard case of study to determine which is the optimum distance between the transducers.

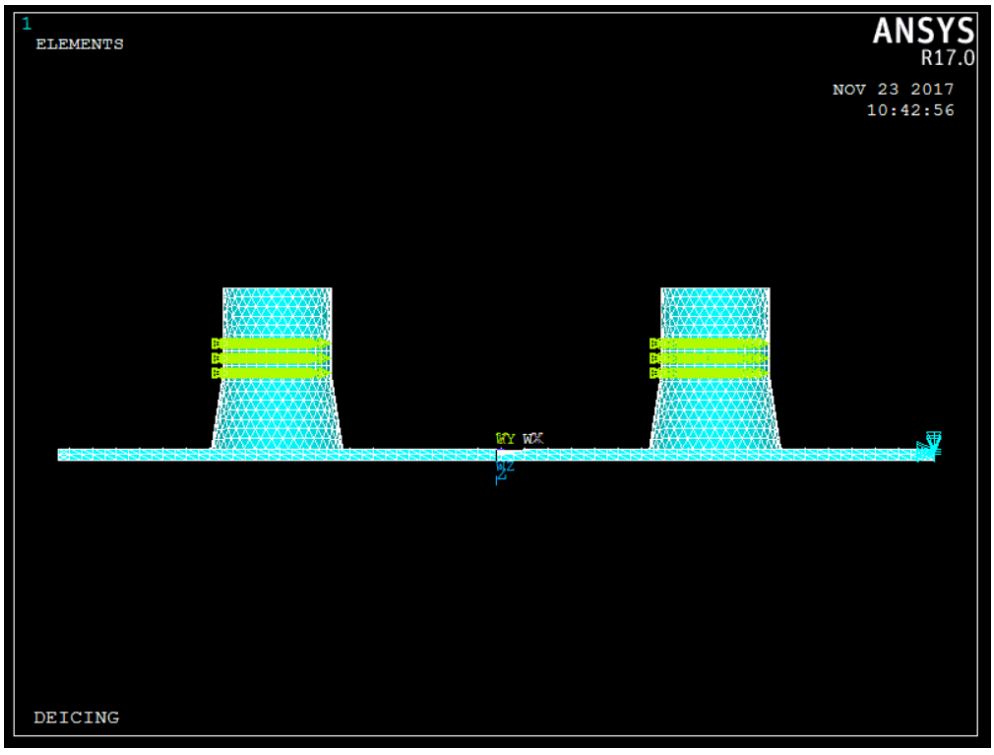

Figure 15. ANSYS simulation body

VI.1.2 Geometry

As it can be seen in the picture, it is developed a laminar rectangular plate where the two transducers are set. Besides, it is mandatory to define and decide the different properties of the involved elements for this case of study. Like the Young modulus, the Poisson ratio, the density, permittivity of the different elements of the system like the ice, the steel in the transducers, the materials of the different parts of the piezoelectric… Also, the physical properties of the elements had to be set in order to determine our case of study.

To see how the distance between the transducers affects the final results, by using the formula [14], the parameters of the composite and the ice layer will be set.

The theory and the results of shear forces can be calculated by the ANSYS software. All of them use the shear forces caused by ultrasonic waves to remove the ice layer.

The element of study is a composite laminar plate of 200*300 mm with two ceramic transducers (PZT-4), as it is showed in the figure 16, experimentally done at a temperature of -15^{o}C.

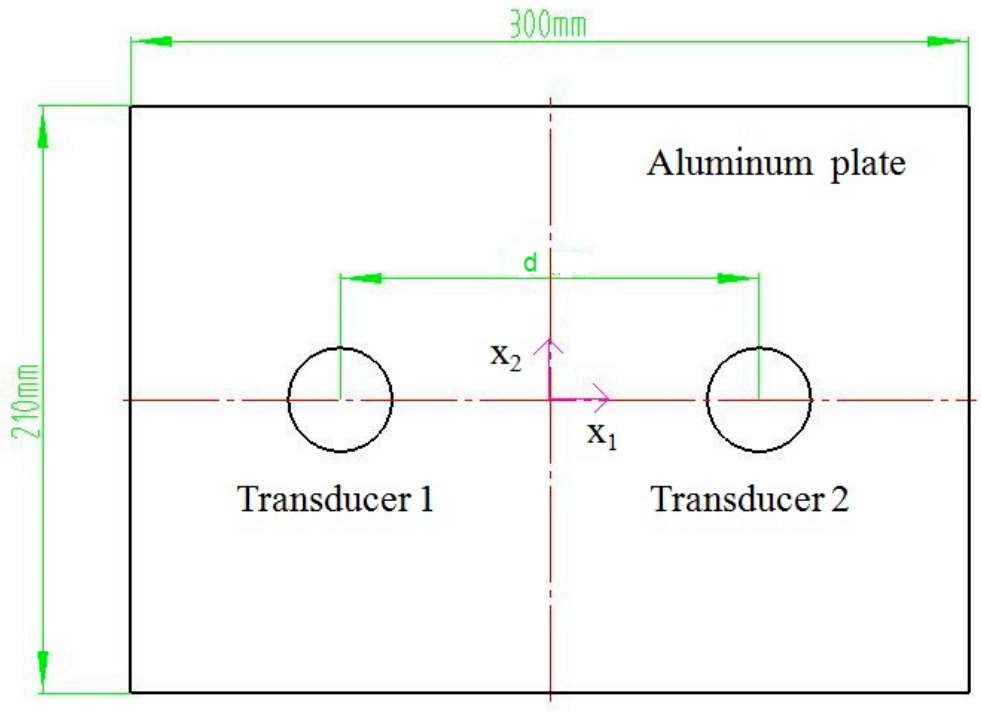

Figure 16. Laminar plate measurement properties

Two piezoelectric wafers are meshed by using SOLID5, composite plate is meshed by Solid 95, and ice layer is meshed by using SOLID45. Two thin electrode slices are added to the upper and the lower surface of piezoelectric wafer respectively, the upper surface is the positive electrode, and the lower surface, connected to rectangle composite plate, is the negative electrode. The applied voltage to the positive electrode is 100 V, the voltage applied to the negative electrode is 0 V.

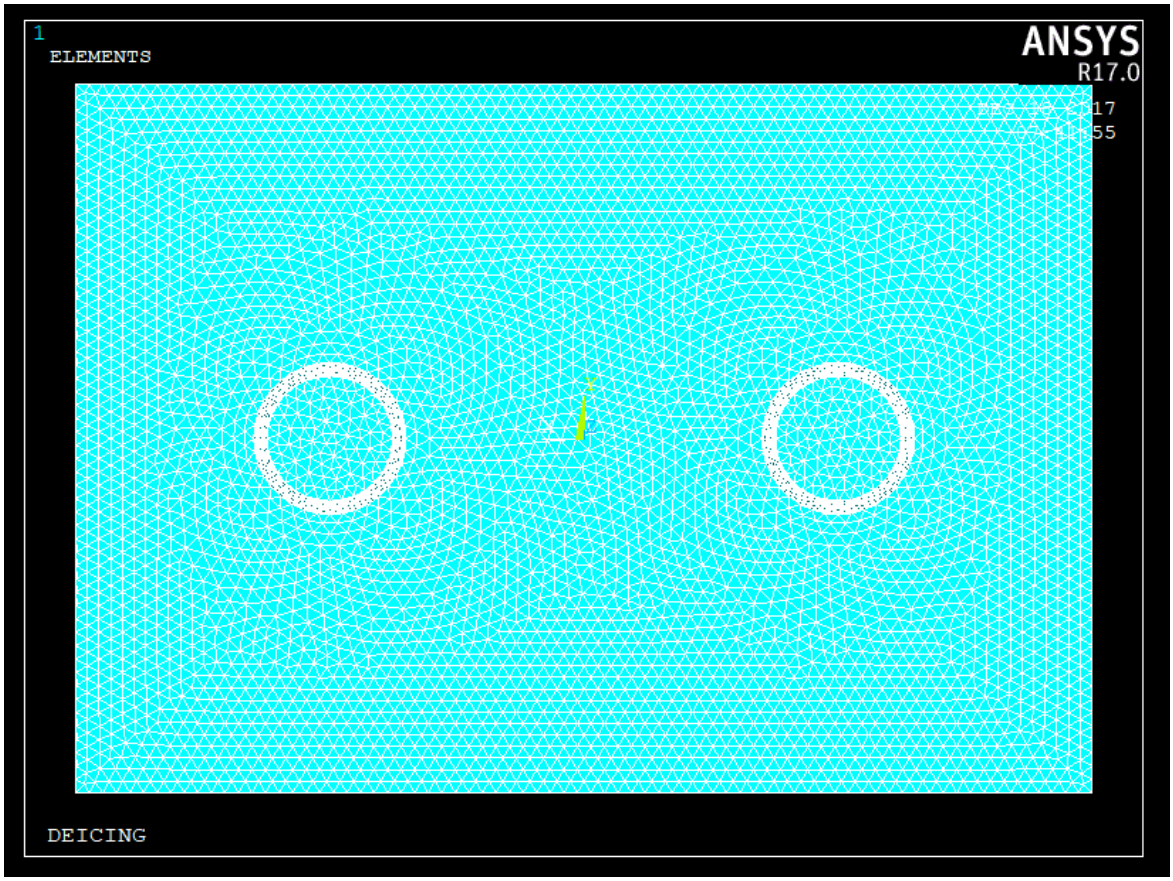

Figure 17. ANSYS laminar plate and two transducers

VI.1.3 Transducer Properties

The properties of the transducer correspond to the material parameters of PZT-4 and are showed below

PROPERTY	MEASURE
Diameter of the piezoelectric disc	0.037m
Thickness of the piezoelectric disc	0.005 m
Length of substrate plate	0.3 m
Width of the substrate plate	0.21 m
High of the substrate plate	0.002 m
Diameter of the piezoelectric disc	0.037 m

Table 1. Transducer properties

Density:

$\rho = 7750\ kg/m^3$

Poisson's Ratio:

$v = 0.3$

Piezoelectric Matrix:

$$\epsilon_{T11} = 804.6$$
$$\epsilon_{T33} = 659.7$$

Relative Permittivity:

$e_{33} = 14.1\ C/m^2$
$e_{13} = -4.1\ C/m^2$
$e_{15} = 10.5\ C/m^2$

Elastic Matrix:

$C_{E11} = 13.2 * 10^7$ N/ m^2
$C_{E12} = 7.1 * 10^{10}$ N/ m^2
$C_{E13} = 7.3 * 10^{10}$ N/ m^2

$C_{E22} = 13.2 * 10^{10}$ N/ m^2
$C_{E23} = 7.3 * 10^{10}$ N/ m^2

$C_{E33} = 11.5 * 10^{10}$ N/ m^2

$C_{E44} = 3 * 10^{10}$ N/ m^2

$C_{E55} = 2.6 * 10^{10}$ N/ m^2

$C_{E66} = 2.6 * 10^{10}$ N/ m^2

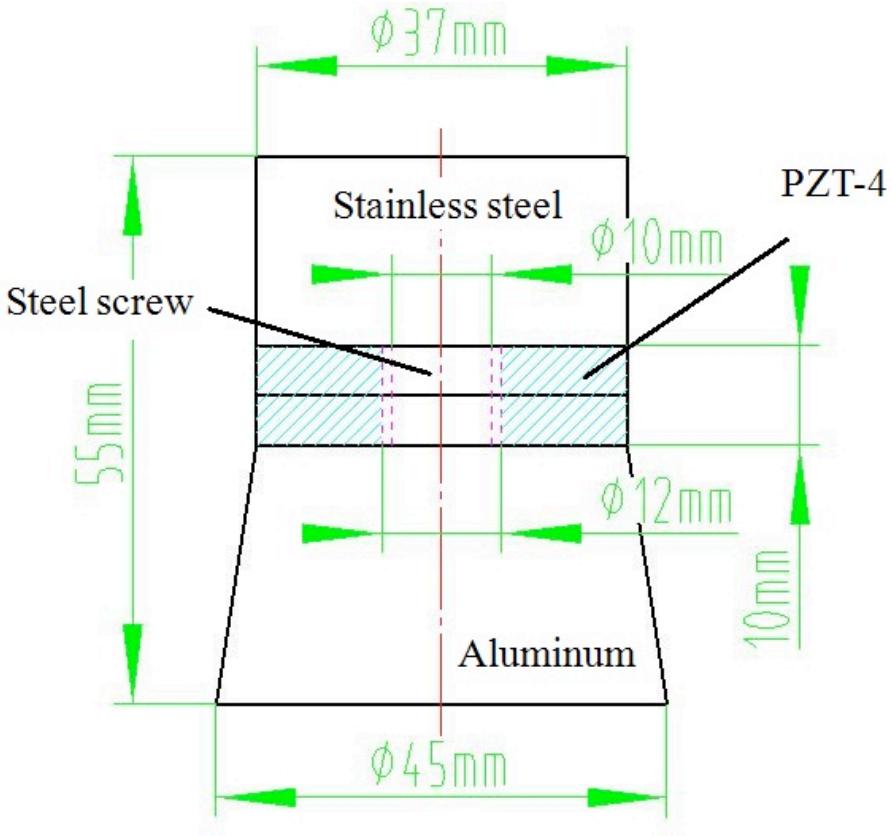

Figure 18. PZT-4 measurement properties

VI.1.4 Composite Properties

The composite plate was made of carbon fiber reinforced polyester matrix composite of 18 layers with orientation distribution along the plate thickness ($\pm 45^{o}$) where each layer has a thickness of 0.12 mm.

The properties of the composite are:

Elastic Modulus:

$E_1=120*10^9$ Pa
$E_2=1.9*10^9$ Pa
$E_3=1.9*10^9$ Pa

Shear Stress:

$G_{12}=G_{23}=G_{13}=4.8*10^9$ Pa

Poisson's Ratio:

$v_{12}=v_{23}=v_{13}=0.3$

Density

$\rho=1.61$ kg*m^{-3}

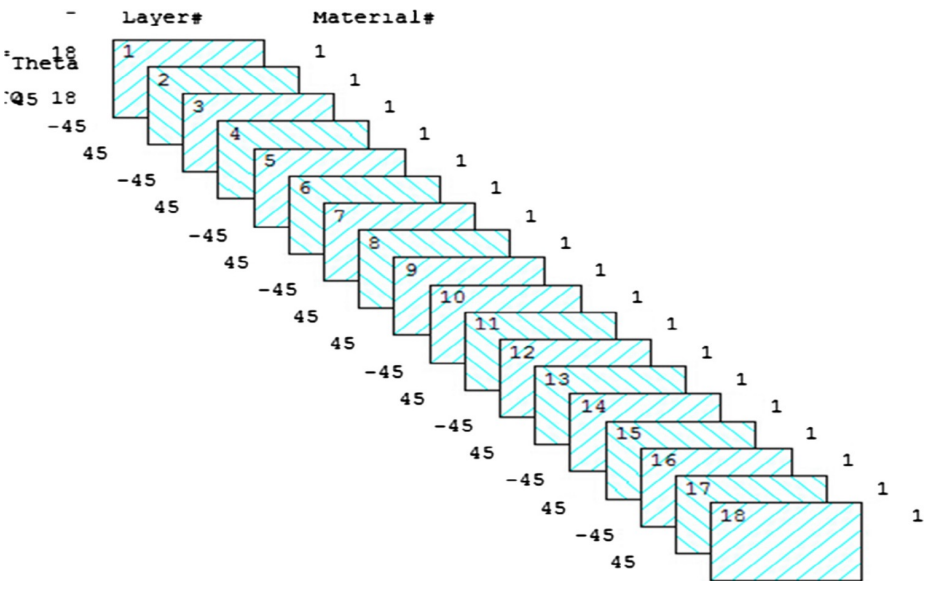

Figure 19. Composite layers and distribution

VI.1.5 Ice Layer properties

The properties of the ice layer are:

Length of the ice
L = 0.3 m

Height of the ice
Z = 0.003 m

Elastic Modulus
E = 6 GPa

Poisson's Ratio
v =0.3

Density
ρ = 0.913 kg*m^{-3}

VI.1.6 Case of Study

According to the objective of this project and taking into account the dispersion of the frequency, it was obtained the following distances between the transducers.

Each case will be one case of study and it will be simulated by ANSYS. The different stresses between planes, the total displacement and the total stress will be performance in order to study the possibility of ice breaking using the optimal distance between the two transducers.

N	Distance (Cm)	Ap.(cm)
1	0.04	0.04
2	0.066666667	0.07
3	0.093333333	0.09
4	0.12	0.12
5	0.146666667	0.15
6	0.173333333	0.17
7	0.2	0.2
8	0.23	0.23
9	0.253	0.25
10	0.28	0.28

Table 2. Cases of study

VI.2 Results

VI.2.1 Optimal Frequency

The optimum frequency range was determinate by simulating with ANSYS several nodes and finding at which value the deicing effect it's optimum.

The results show that the variation of stress with ultrasonic excitation frequency determine the optimal frequency for reach the maximum stress it is equal to 375 kHz. As it can be seen in the following figure:

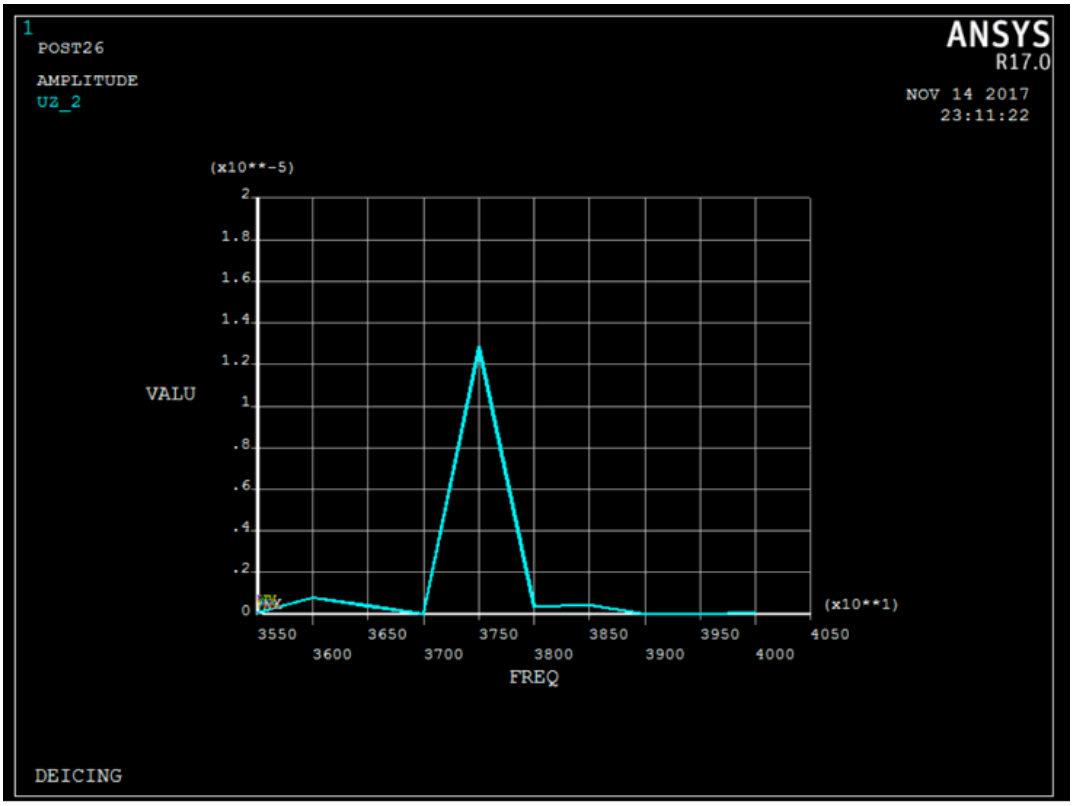

Figure 20. Amplitude-Frequency curve

VI.2.2 Cases of Study: Distance

Once the optimal frequency is obtained, it is possible to simulate with ANSYS and obtain the particular stress of the case of study for the determined frequency.

In the next steps will be showed different studies where the distance of the transducers is modified and how the stress changes also is linked to the distance.

In the next figures is possible to see the stress in plane XY, the total displacement vector sum and the total stress. Just taking a look on the images it is possible to determine the desired results.

VI.2.2.1 Distance 0.25 cm

For the case where the distance between transducers is 0.25 cm, it is possible to see how the maximum value of stress rounds the value $40*10^4$ Pa.

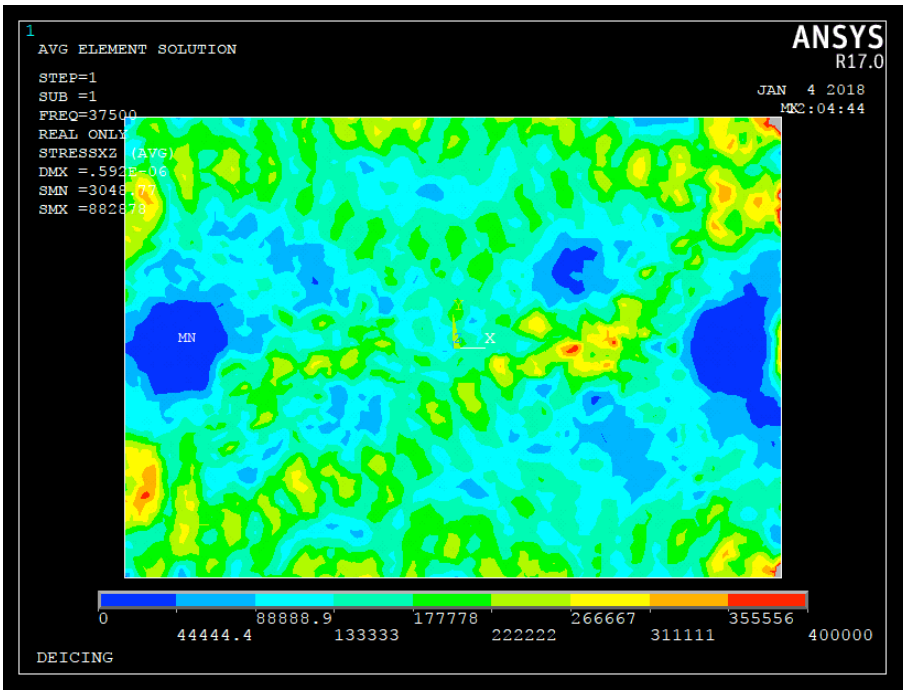

Figure 21. Distance 0.25 cm total peak stress

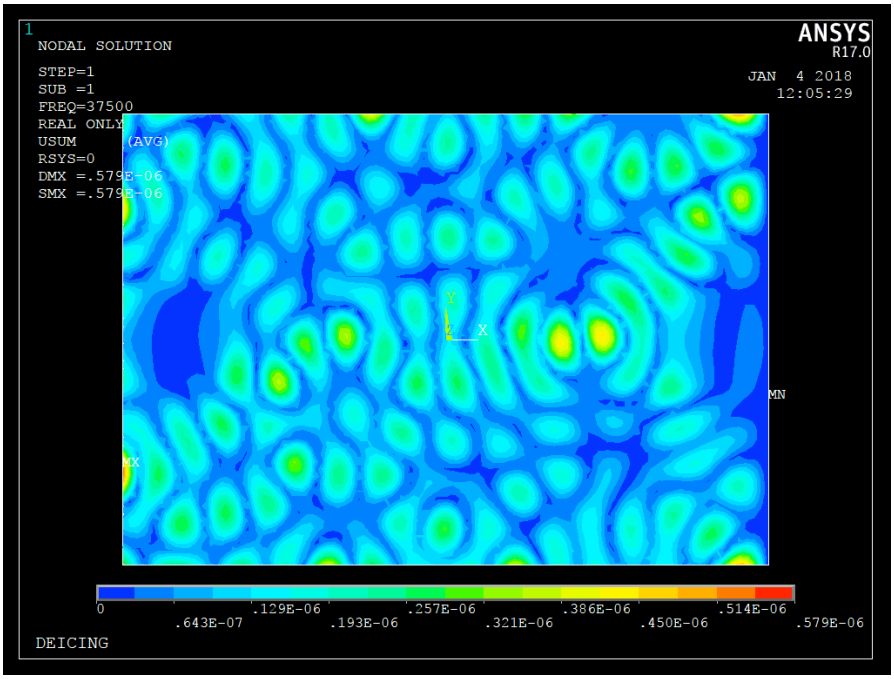

Figure 22. Distance 0.25 cm total displacement

VI.2.2.2 Distance 0.23 cm

For the case where the distance between transducers is 0.23 cm, it is possible to see how the maximum value of stress rounds the value $13*10^4$ Pa.

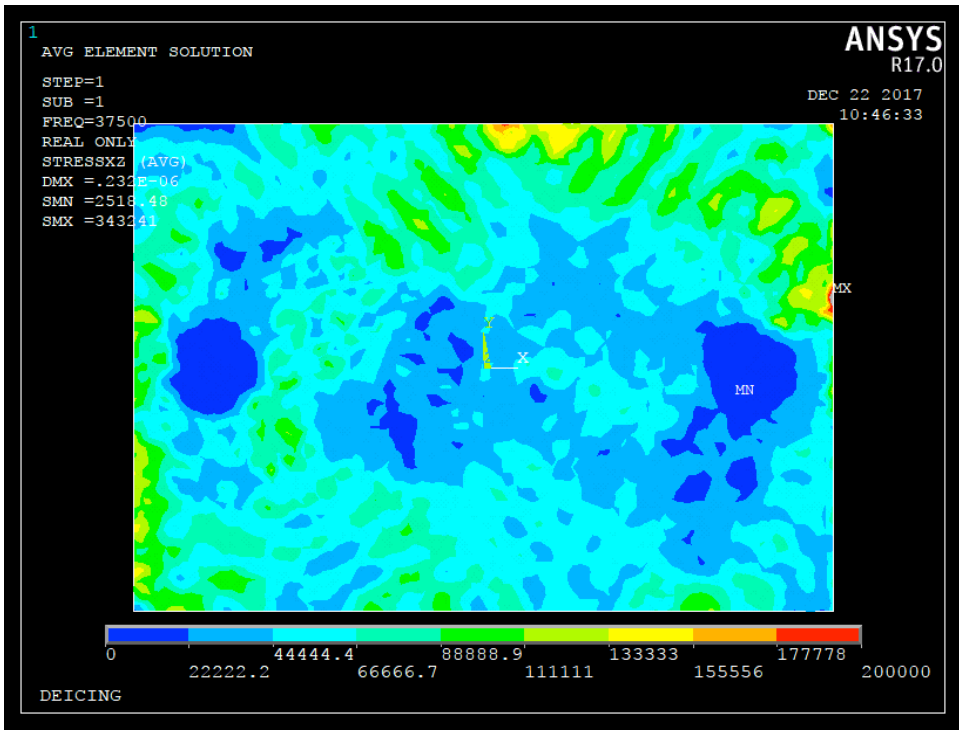

Figure 23. Distance 0.23 cm total peak stress

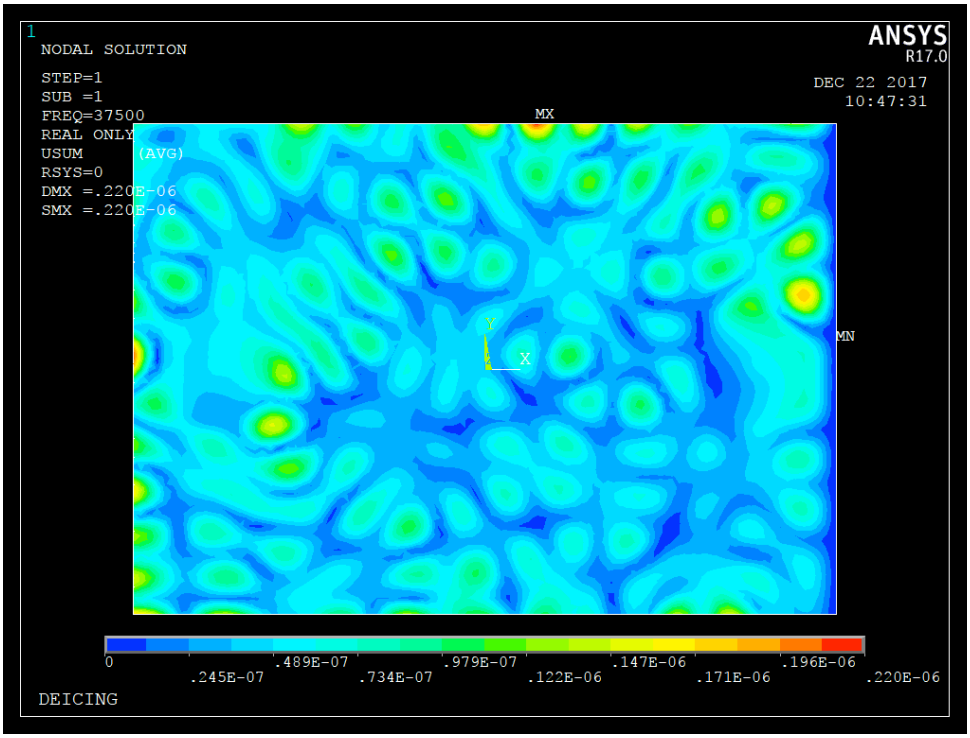

Figure 24. Distance 0.23 cm total displacement

VI.2.2.3 Distance 0.20 cm

For the case where the distance between transducers is 0.20 cm, it is possible to see how the value of stress it reaches maximum value of stress is around the value $10*10^4$ Pa.

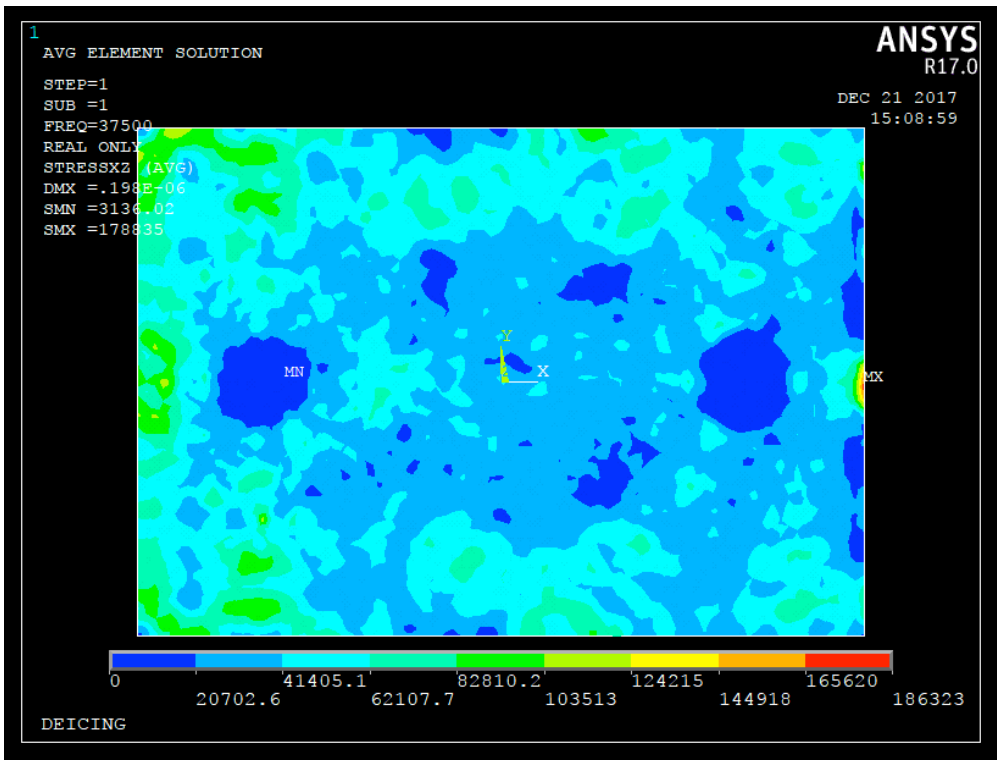

Figure 25. Distance 0.20 cm total peak stress

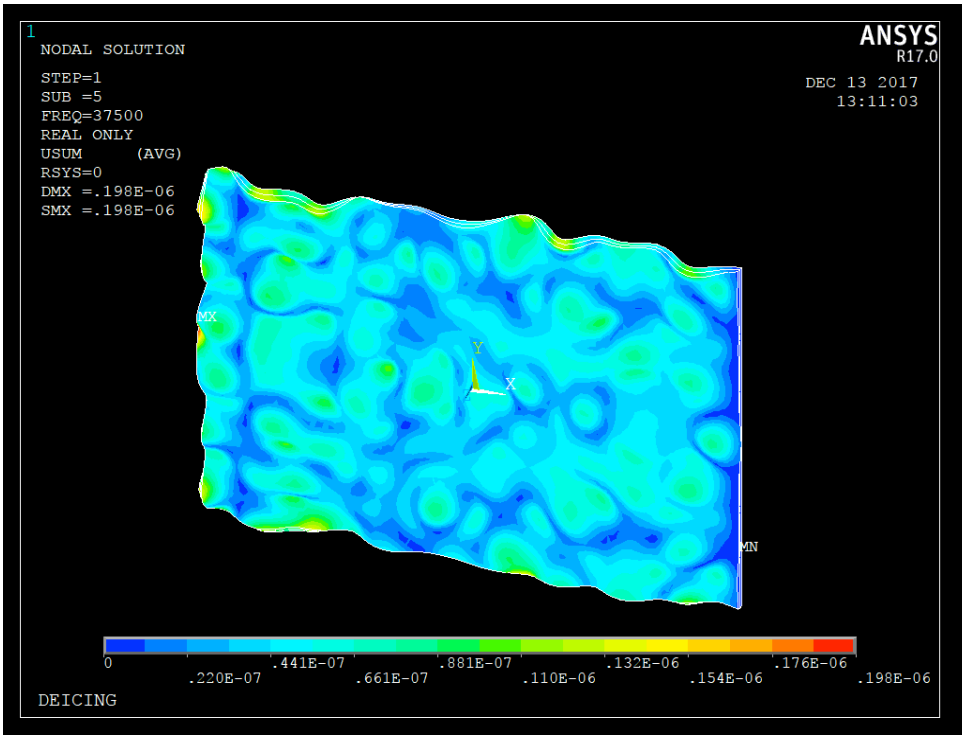

Figure 26. Distance 0.20 cm total displacement

VI.2.2.4 Distance 0.17 cm

For the case where the distance between transducers is 0.17 cm, it is possible to see how the maximum value of stress rounds the value $46*10^4$ Pa.

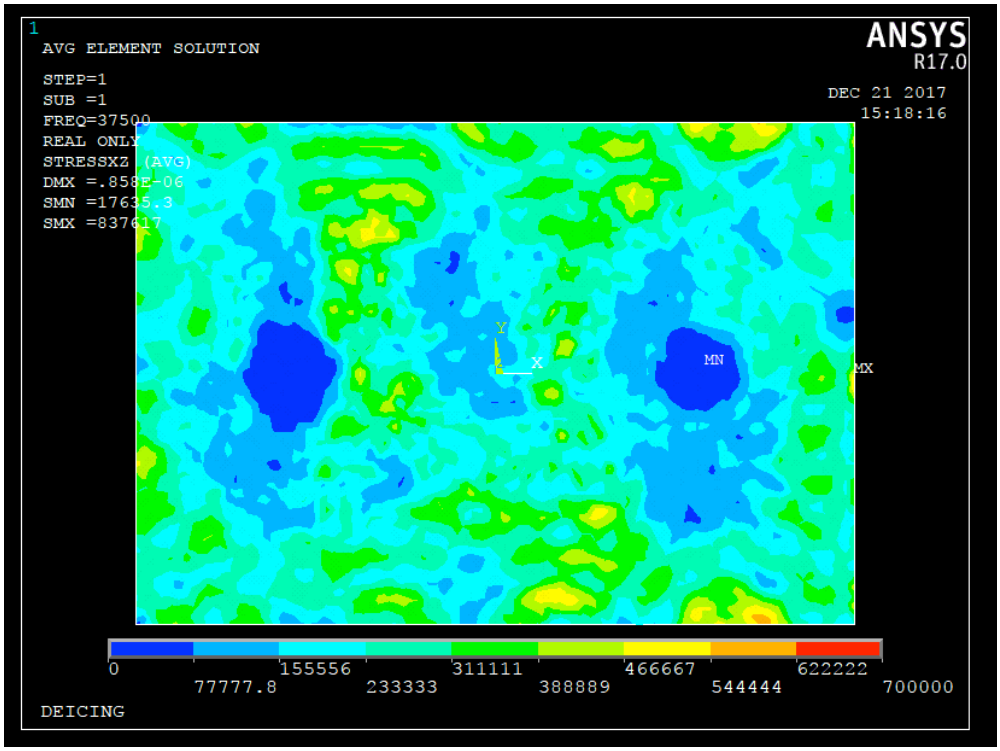

Figure 27. Distance 0.17 cm total peak stress

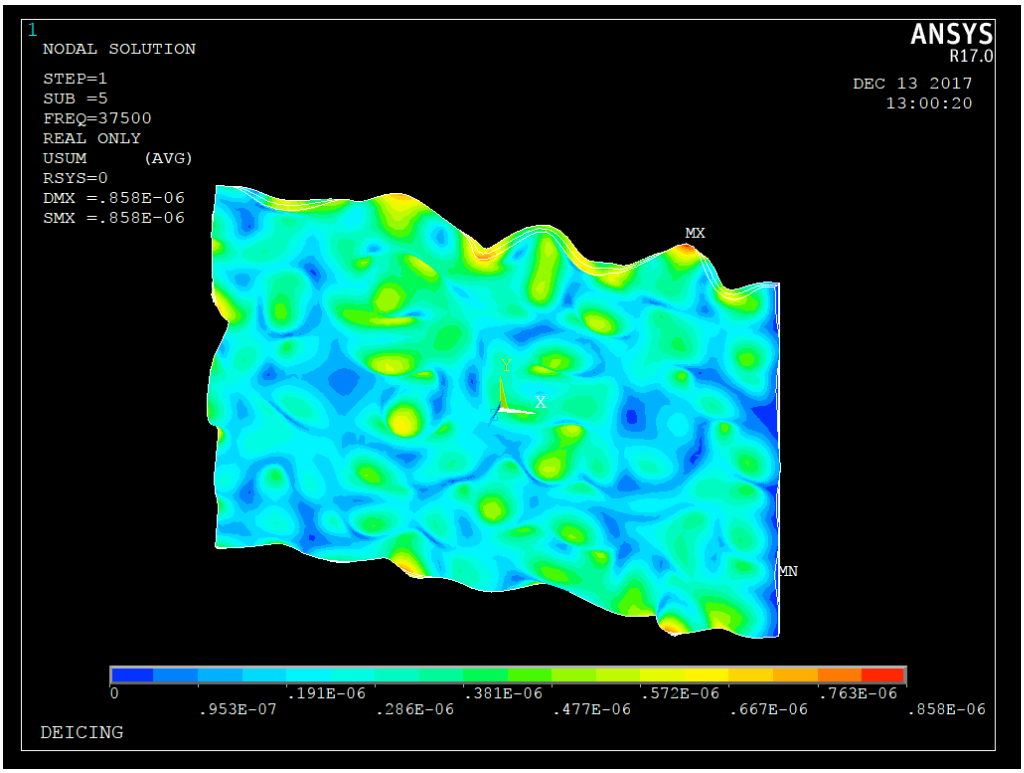

Figure 28. Distance 0.17 cm total displacement

VI.2.2.5 Distance 0.15 cm

For the case where the distance between transducers is 0.15 cm, it is possible to see how the maximum value of stress rounds the $33*10^4$ Pa.

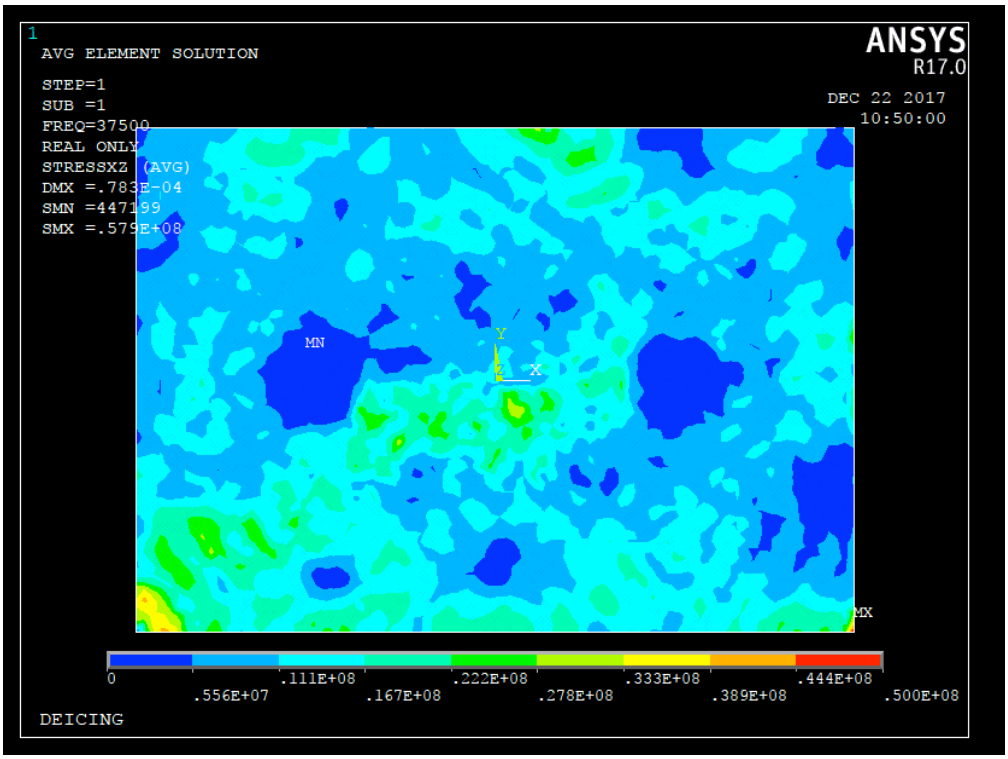

Figure 29. Distance 0.15 cm total peak of stress

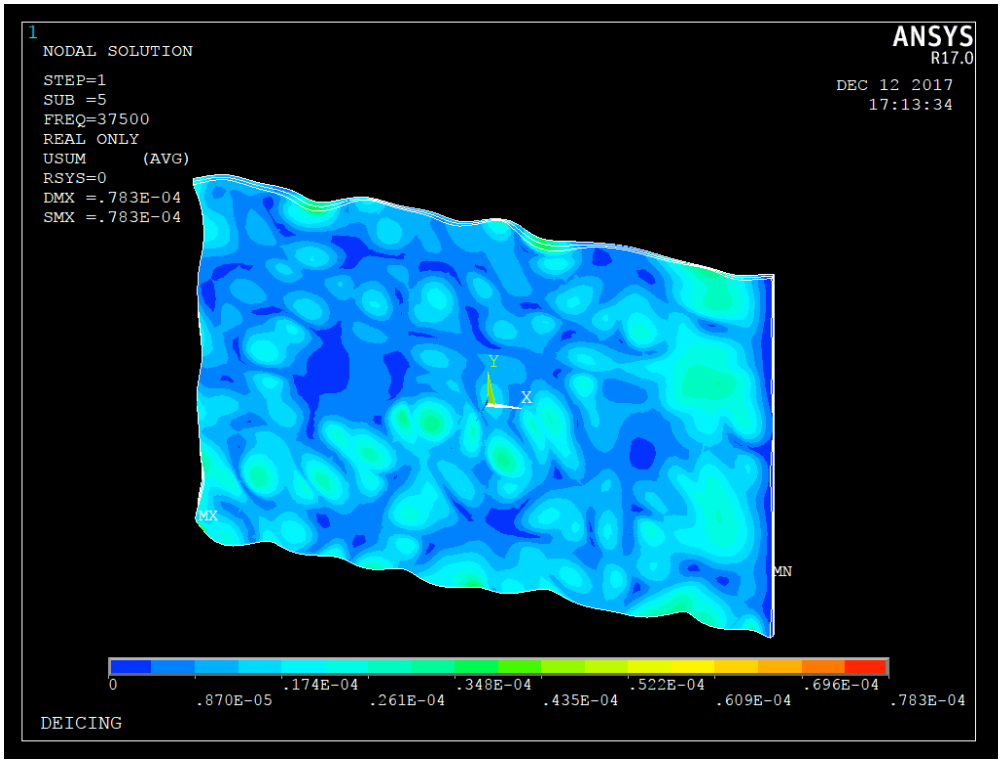

Figure 30. Distance 0.15 cm total displacement

VI.2.2.6 Distance 0.12 cm

For the case where the distance between transducers is 0.12 cm, it is possible to see how the maximum value of stress rounds the value $10*10^4$ Pa.

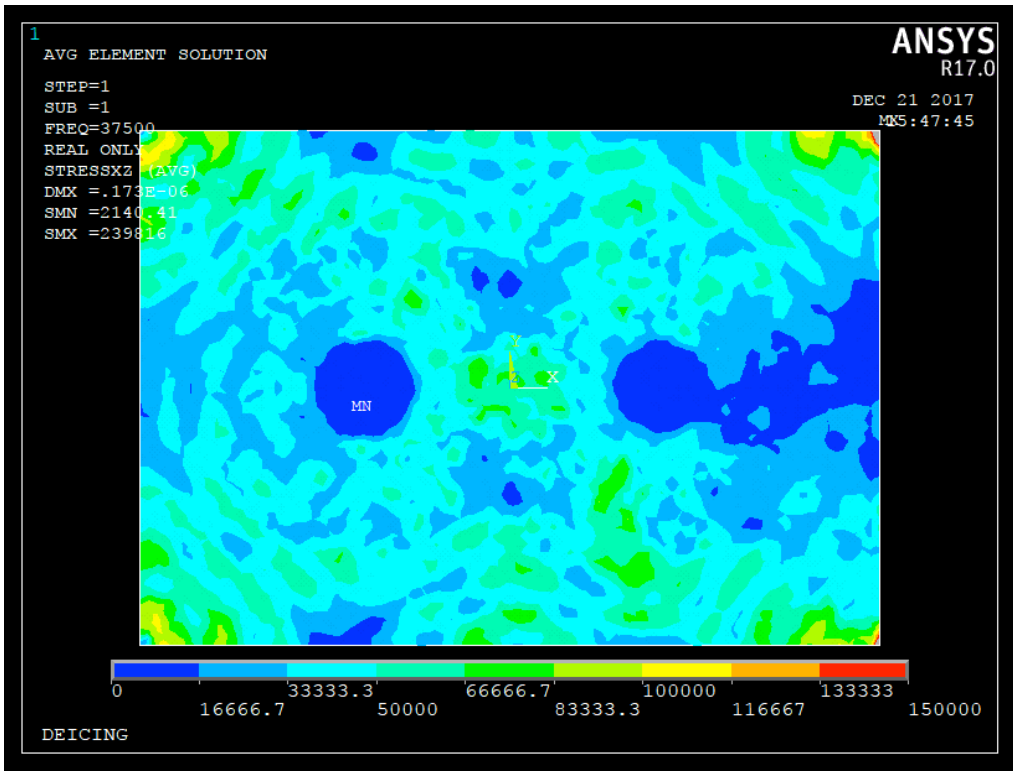

Figure 31. Distance 0.12 cm total peak stress

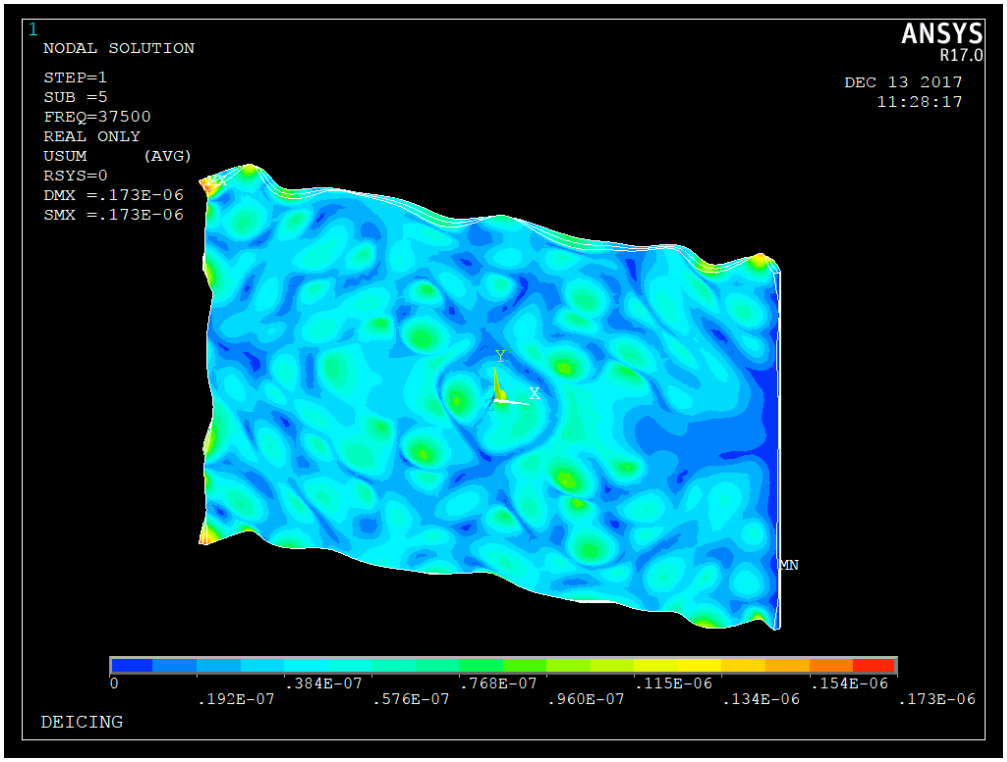

Figure 32. Distance 0.12 cm total displacement

VI.2.2.7 Distance 0.09 cm

For the case where the distance between transducers is 0.09 cm, it is possible to see how maximum value of stress is around the value $22*10^4$ Pa.

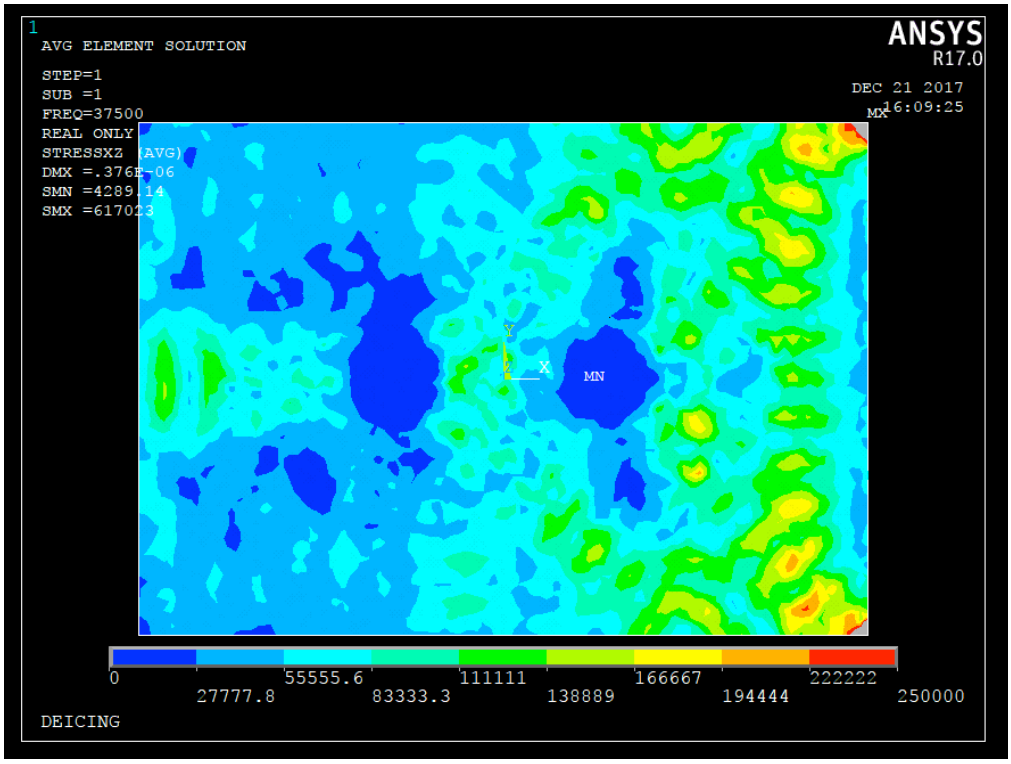

Figure 33. Distance 0.09 cm total peak of stress

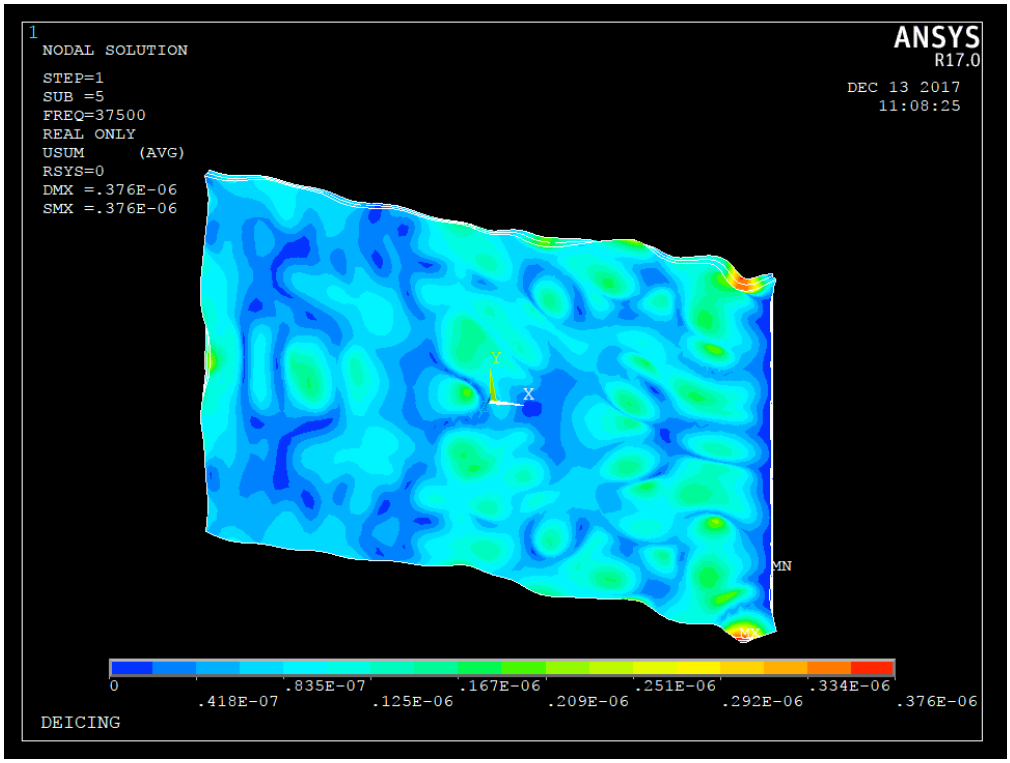

Figure 34. Distance 0.09 cm total displacement

VI.2.2.8 Distance 0.07 cm

For the case, where the distance between transducers is 0.07 cm, it is possible to see how the maximum value of stress rounds the value $53*10^4$ Pa.

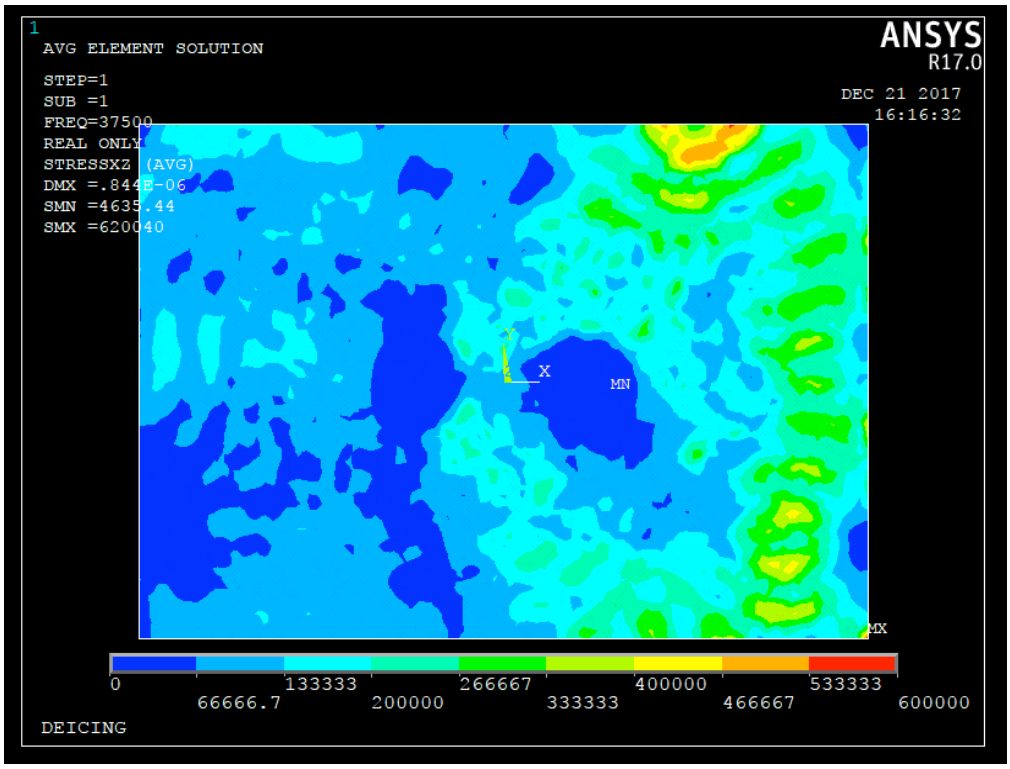

Figure 35. Distance 0.07 cm total peak stress

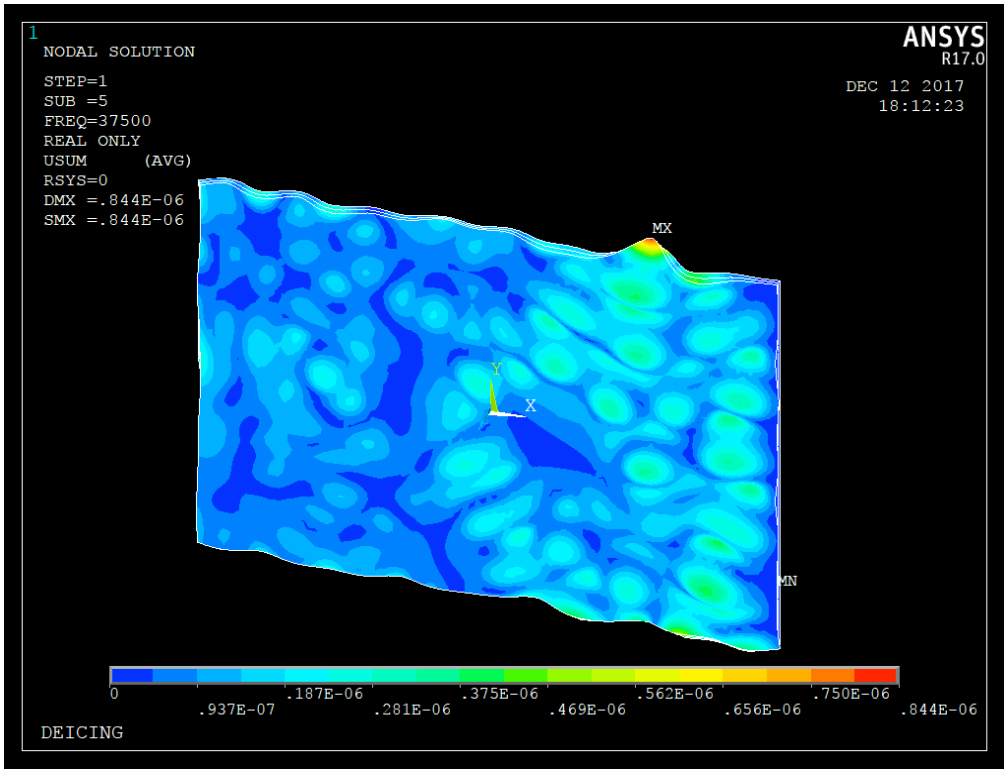

Figure 36. Distance 0.07 cm total displacement

VI.2.2.9 Distance 0.05 cm

For the case where the distance between transducers is 0.05 cm, it is possible to see how the maximum value of stress rounds the value $90*10^4$ Pa.

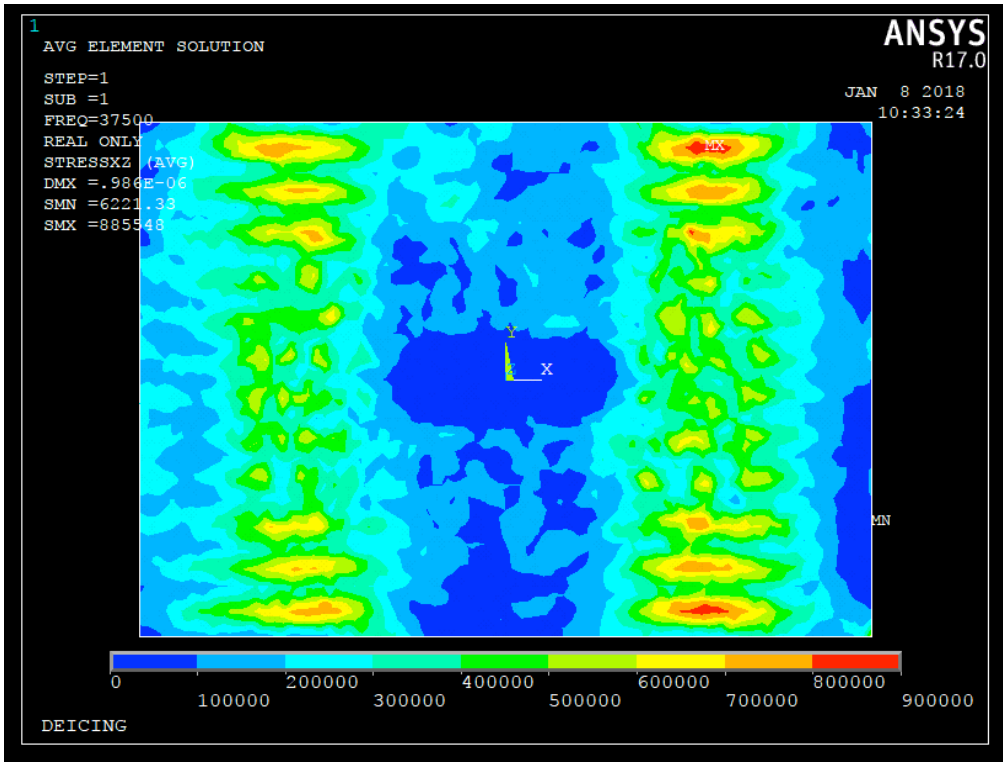

Figure 37. Distance 0.05 cm total peak stress

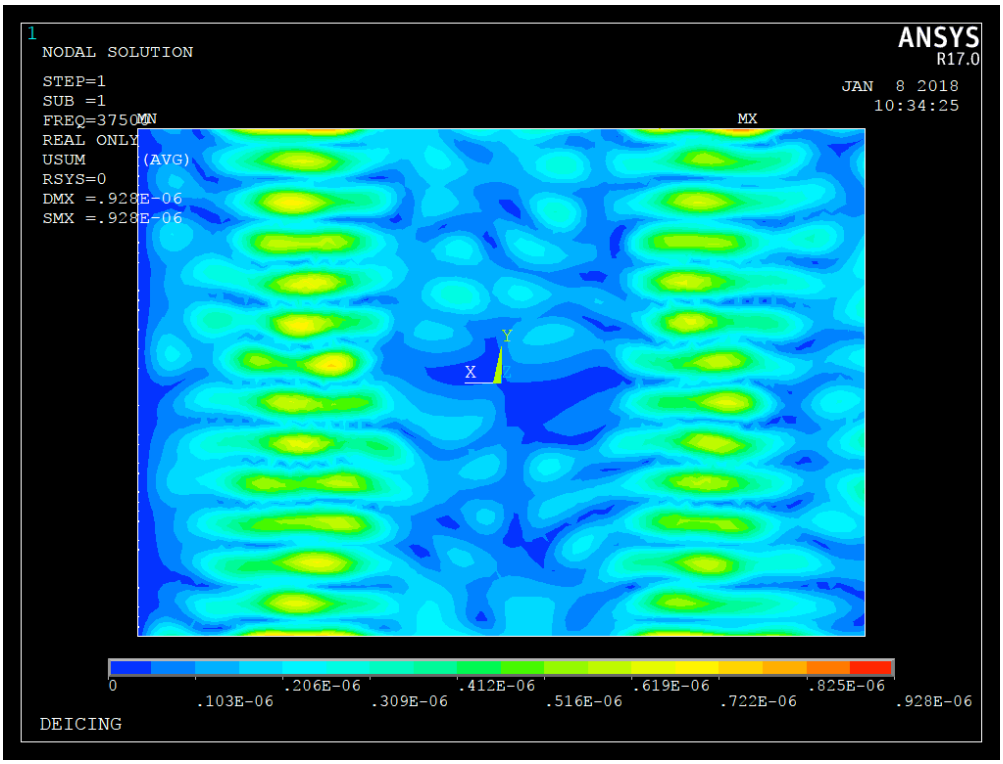

Figure 38. Distance 0.05 cm total displacement

VI.3 Relation between stress and distance

In the following table is shown the results of ANSYS:

Distance (cm)	Peak Stress(MPa)
0.25	0.35
0.23	0.15
0.20	0.10
0.17	0.46
0.15	0.33
0.12	0.10
0.09	0.22
0.07	0.53
0.05	0.90

Table 3. Peak stress distances

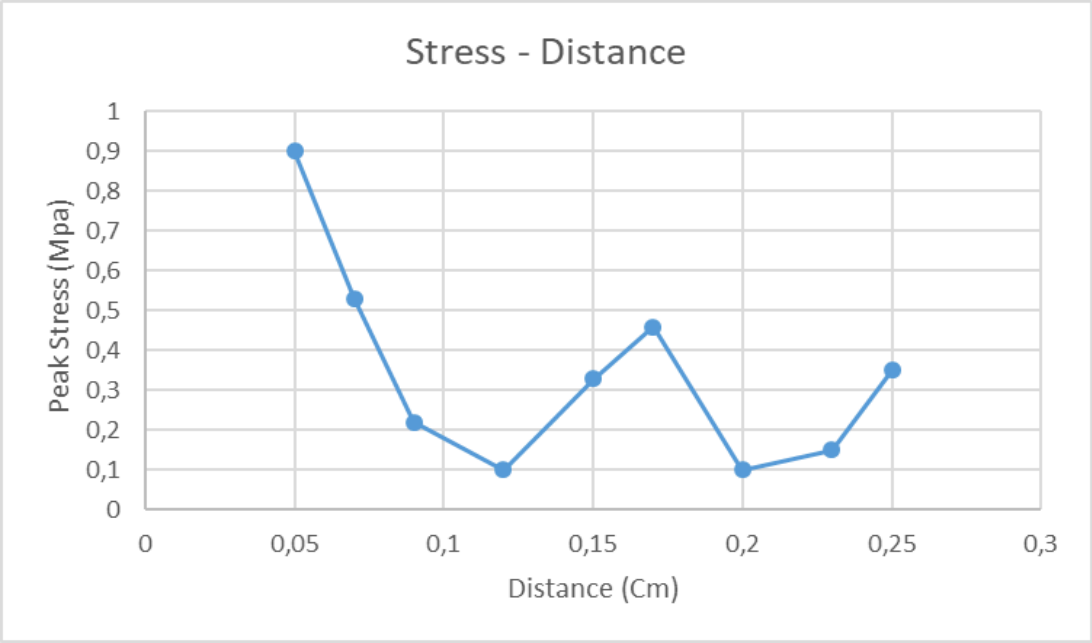

Figure 39. Stress-distance relation

According with the study done by Mr Wang and Mr Xu; "*An effect assessment and prediction method of ultrasonic de-icing for composite wind turbine blades*", the maximum adhesive strength between composite plates and ice layer is around 0.4 MPa. As it can be seen in the figure and table above, the only points that achieve a maximum stress peak greater than 0.4MPa correspond to the distances 0.17, 0.07 and 0.05.

VII Results analysis

VII.1 Distance - Stress Equation

The numerical results show that the correlation between the distance where the transducers are settled and the total peak stress generated is neither linear nor exponential function. In fact, these results seem to follow a damped wave equation as in the figure below.

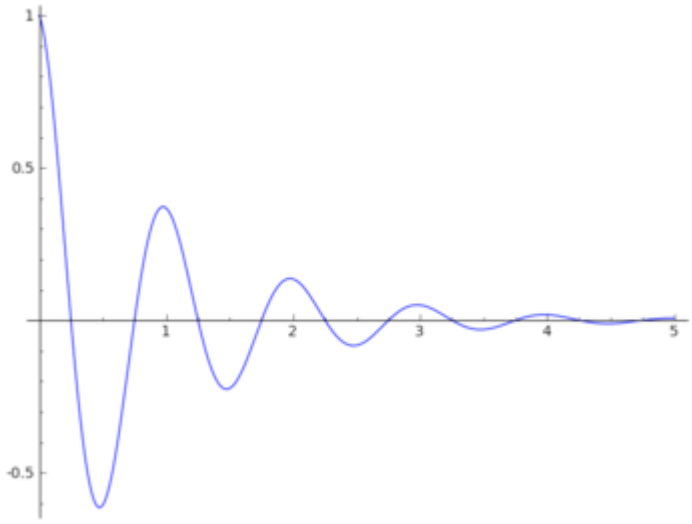

Figure 40. Damped wave

A priori, this means that best locations will not be best as the transducers are closer or further from each other. The best positions that can reach one value of stress enough to break the ice will be allocated in the maximums of the damped wave and these points will be decreasing slowly into a constant as long as you tent to the infinity.

In the three distanes that reach the 0.4MPa, it is able to observe that the stress that suffers the plate is really different between them.

Distance (cm)	Peak Stress(MPa)
0,17	0,46
0,07	0,53
0,05	0,90

Table 4. Distances that may break the ice

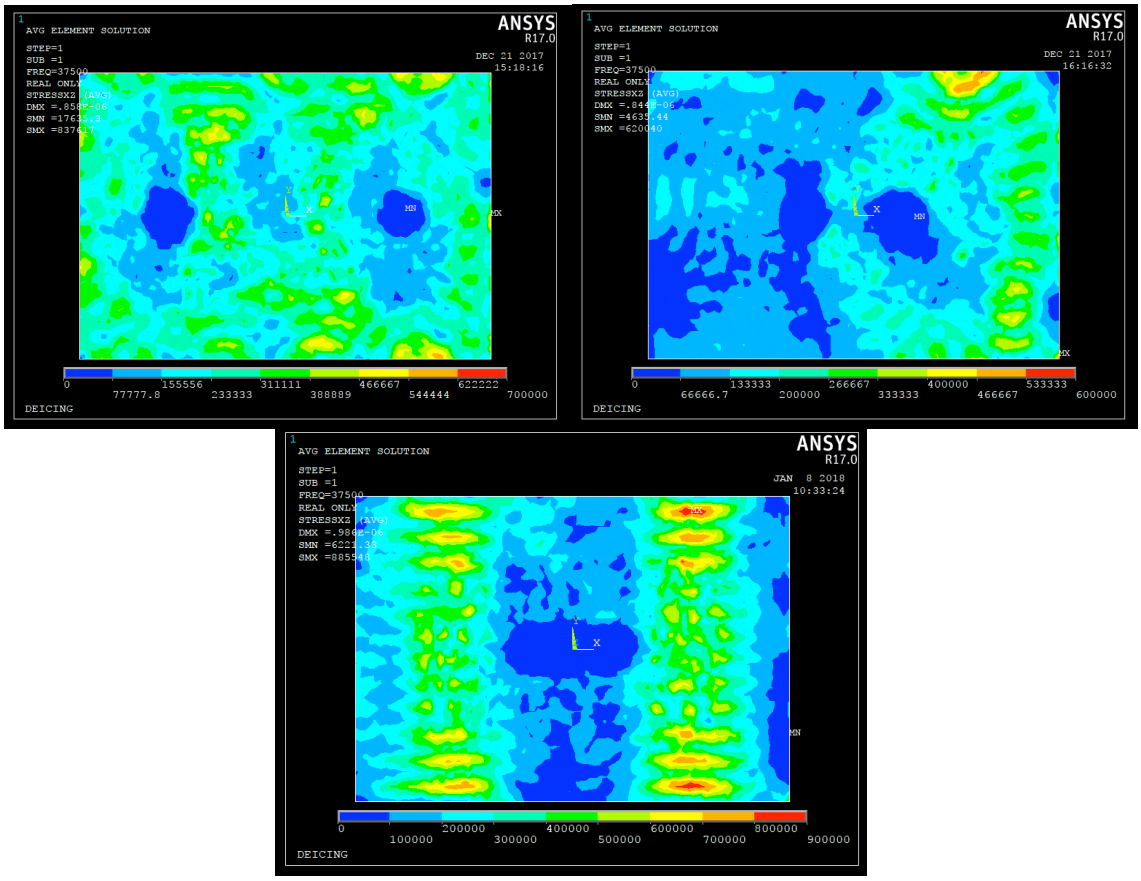

Figure 41. From right to left and from up to down, stress that corresponds to distance 0.17 cm, 0.07 cm and 0.05 cm

As it is observed in the images above, the distances 0.05 cm and 0.07 cm have greater peaks of stress than in 0.17 cm. However, in the figures we can see that stresses bigger than 0.4MPa are localized in the right of the plate when the transducers are at 0.07 cm and in two stripes when the transducers are at 0.05 cm. These cases will be not capable to de-ice the whole plate, instead they have the big peaks of stressed. For the distance of 0.17 cm between the transducers it is easy to observe that the whole plate suffers stresses around 0.4MPa making the configuration the most viable to de-ice in a real case.

VII.1Observations

This experiment and the results obtained are just a research to establish some criteria at the time to set the distance between transducers.

To set an exact value the result could be different for real cases. The distance between transducers depends of several factors as it is explained before; like the material where you set the transducers, the type of transducer, the shape of the surface contact, the temperature, the thickness of the ice, the power supplied and so far.

The results obtained are just viable for this particular study and should be taken into account for future experimental researches. Wrap it in all that means, there are many different distance where you can set the transducers to break the ice, if you just consider the distance between them just is needed to check the value where the ice breaks and choose the most far point that reach that stress.

However, in the other hand, if you change the initial conditions the optimal distances between the transducers may vary. Changing these initial variables will be interesting for future studies too.

VIII Conclusions

The main purpose of this project it was investigate the behavior of the interaction between two transducers in a flat laminar plate in order to break an ice layer and check the feasibility to use it like a new aeronautical de-icing system. Also made an aeronautical assessment of the implementation and usability of the ultrasonic deicing system.

First it was compared the system between the currently competitors like active-passive deicing and anti-icing systems.
This concluded that the ultrasonic deicing system own a big potential in the future of the aeronautical de-icing, because the system consumes less amounts of energy, it has a low cost and its easy replacement and maintenance, in comparison with the competitor's systems.
As an observation, the currently bad points of the ultrasonic de-icing system and some of the main reasons why it is not yet implemented in the aeronautical industry are principally that it is needed so many transducers and also that they still being too heavy to be carried by the interface of the airplane. Furthermore, adding that the aeronautical industry takes many time and large processes to add new technologies in the its environment makes that the solution still not available, but with time and some upgrades this could change in the close future.

Secondly, it was proposed a particular case of study, with particular initial values, to check the previous experiments and the feasibility to apply these kind of systems.
It was carried and experimental simulation by analytical software ANSYS where it was developed a flat laminar composite plate, with two transducers type PZT-4 where it was pretended to break an ice layer of 3 cm of thick at a temperature of -15^{o}C. Then it was simulated several different distance between the transducers.

The results showed for this particular case that the distance between transducers don't follow a common tendency, it suits the behavior to a damping wave equation where it reaches some maximum of stress at the beginning where the distance is the closest one and later in measure that you increase the distance between finds some distances where the value of stress reaches some peaks of stress that are going decreasing in sequence.

This conclude that for the particular case where the unique variable is the distance and all the other parameters are constants. The optimum and the more efficient distance between transducers is at 0,17 cm. Where the stress reached at that distance seems to be enough for break the ice theoretically (0,47 MPa). However, we think that in a real case it will be not break because, as we can see in the figures obtained by ANSYS, the values of the whole plate rounds the 0.4MPa by little and in real cases will be losses for sure.

As it was mentioned before this results only suits for that particular experiment or case of study because there are many factors that can affect the optimum position of the transducers, as type of materials used, temperature, ice layer…
But all of this parameters where not included in our research. Just the distance.

We would like to remark the importance of simulate within informatics software all this previews calculations and hypothesis what result in a cheapening in the cost of build and resources like prototypes or devices.

To conclude, there are some topics that will be improved and updated in the future, like reduce cost, efficient piezoelectric, mini-size materials, application in real aircraft structure, electronic control systems, better designs etc.
Once all these topics they are solving the ultrasonic deicing system it will be a for his characteristics a suitable technology for aeronautical engineering in the near future.

IX References

[1] **A light lithium niobate transducer for the ultrasonic de-icing of wind turbine blades**. Zhenjun Wang, Yuanming Xu, Fei Su, Yibing Wang

[2] **An effect assessment and prediction method of ultrasonic de-icing for composite wind turbine blades,** Yibing Wang, Yuanming Xu, Yuyong Lei**,** School of Aeronautic Science and Engineering, Beihang University, Beijing,100191, China

[3] **"Aircraft Icing,"** Gent, R.W., Dart, N.P., and Candsdale, J.T Philosophical Transactions of the Royal Society of London Series A, Vol. 358, 2000

[4] **Analysis of piezoelectric ice protection systems combined with ice-phobic coatings,** Valérie Pommier-Budinger1, Université de Toulouse, Institut Supérieur de l'Aéronautique et de l'Espace, 31055 Toulouse, France Marc Budinger 2, Université de Toulouse, Institut Clément Ader, INSA Toulouse Toulouse, 31077, France *and* Nick Tepylo 3, Xiao Huang 4 Carleton University, Dept. of Mechanical and Aerospace Engineering, Canada.

[5] **Anti-icing and de-icing techniques for wind turbines: critical review,** Olivier Parent, Adrian Ilinca, Cold Regions Sci. Technol. 65 (2011) 88e96.

[6] **De-icing of multi-layer composite plates using ultrasonic guided waves**, Yun Zhu, J.L. Palacios, Joseph L. Rose, Edward C. Smith. AIAA 2008-1862.

[7] **Experimental study on ultrasonic effect in oil reservior**, Wang Ruifei, Sun Wei, You Xiaojian, Zhang Rongjun, Cheng Hua, Pet. Geol. Exp. 37 (2) (2006) 449e454.

[8] **Instantaneous Deicing of Freezer Ice via Ultrasonic Actuation**. Jose Palacios1, Edward Smith2, and Joseph Rose3,*The Pennsylvania State University, University Park, PA, 16802*

[9] **Numerical Simulation and Experiment of the Piezoelectric De-Icing System**, ZHU Yongjiu[1, a], LI Qingying

[10] **Numerical simulation and experimental validation of ultrasonic de-icing system for wind turbine blade.** Congbo Yin, Zhendong Zhang, Zhenjun Wang, Hui Guo a College of Mechanical Engineering, University of

Shanghai for Science and Technology, Shanghai 200093, China b College of Automobile Engineering, Shanghai University of Engineering Science, Shanghai 201620, China.

[11] ***Piezoelectric Deicing System for Rotorcraft.*** Available from: https://www.researchgate.net/publication/312530677_Piezoelectric_Deicing_System_for_Rotorcraft

[12] **Progress on ultrasonic guided waves de-icing techniques in Improving aviation energy efficiency**.Yibing Wang, Yuanming Xu□, Qi Huang School of Aeronautic Science and Engineering, Beihang University, Beijing 100191, China.

[13] **Ultrasonic de-icing of wind-tunnel impact icing**, Jose Palacios, Edward Smith, Joseph Rose, J. Aircr. 48

[14] **Vibration de-icing method with piezoelectric actuators on flat Aluminum plate**, BAI Tian[1], ZHU Chunling[1], MIAO Bo[1], LI Qingying[2], ZHANG Quan[3]

X Acknowledge

We would be pleased to dedicated a few lines to Mr. Yuanming Xu from the School of Aeronautic Science and Engineering, Beihang University in Beijing for give us the opportunity to realize this project and introduce us in this cutting edge field in the aeronautics. Also, we are really grateful for his predisposition and all the help he gave us during all the project and for his huge knowledge in this major.

Furthermore, we want to mention Mr. Yibing Wang for all the help and time he provided us and also for the tutorials in the understanding of the simulation software, ANSYS.

We want to recognize also the help provided for the Beihang University, like accommodation, scholarships, lessons, teachers and all the events done to make our exchange comfy.

To end, we want to remark that we are so grateful for the experience and moments lived here that will be impulse our professional career.

XI Annexes

XI.1 ANSYS CODE

```
/PREP7
/TITLE, DEICING
ET,1,SOLID45      !Set element 1，substrate，ice
ET,2,SOLID95      !Set element 1，steel in transducers
ET,3,SOLID5,0     !Set element 3，PZT

MP,EX,1,7E10      !Set Yong's modulus E of material 1，substrate
MP,NUXY,1,.3      !Set Possion ratio of material 1，substrate
MP,DENS,1,2702    !Set density of material 1，substrate

MP,EX,2,6E9       !Set Yong's modulus E of material 2，ice
MP,NUXY,2,.3      !Set Possion ratio of material 2，ice
MP,DENS,2,913     !Set density of material 2，ice

MP,DENS,3,7750    !Set density of material 3，PZT
TB,PIEZ,3         !Set piezoelectric matrix of material 3，PZT
TBDATA,3,-4.1
TBDATA,6,-4.1
TBDATA,9,14.1
TBDATA,9,1.3
TBDATA,14,10.5
TBDATA,16,10.5

MP,PERX,3,804.6       !Set relative permittivity of material 3，PZT
MP,PERY,3,804.6
MP,PERY,3,659.7

TB,ANEL,3           !Set modulus E of material 3，matrix（6×6）symmetry
TBDATA,1,13.2E10,7.1E10,7.3E10 !(1,1),(1,2),(1,3)
TBDATA,7,13.2E10,7.3E10       !□(2,2),(2,3)
TBDATA,12,11.5E10             !□(3,3)□
TBDATA,16,3E10                !□(4,4)□
TBDATA,19,2.6E10              !□(5,5)
TBDATA,21,2.6E10              !□(6,6)

MP,EX,4,200E9     !Set Yong's modulus E of material 4，steel in transducers
```

```
MP,NUXY,4,.3       !Set Possion ratio of material 4
MP,DENS,4,7900     !Set density of material 4

MP,DENS,5,7750     !Set density of material 5,the second PZT disc
TB,PIEZ,5          !Set piezoelectric matrix of material 5
TBDATA,3,4.1
TBDATA,6,4.1
TBDATA,9,-14.1
TBDATA,9,-1.3
TBDATA,14,-10.5
TBDATA,16,-10.5

MP,PERX,5,804.6        !Set relative permittivity of material 5
MP,PERY,5,804.6        □
MP,PERY,5,659.7
□
TB,ANEL,5              !Set modulus E of material 5，matrix（6×6）symmetry
TBDATA,1,13.2E10,7.1E10,7.3E10
TBDATA,7,13.2E10,7.3E10        □
TBDATA,12,11.5E10              □
TBDATA,16,3E10                 □
TBDATA,19,2.6E10               □
TBDATA,21,2.6E10

*SET,R,3.7E-2                  ! diameter of PZT disc (m)
*SET,t,5E-3                    ! thickness of PZT disc
*SET,d,15E-2                   ! distance between 2 transducers
*SET,Lal,300E-3                ! lenth width and high of substrate plate
*SET,Wal,210E-3
*SET,Hal,2E-3
*SET,Lic,300E-3                ! lenth width and high of ice
*SET,Wic,210E-3
*SET,Hic,2E-3

K,1,Lal/2,Wal/2,0              !keypoint of model
K,2,Lal/2,-Wal/2,0
K,3,-Lal/2,-Wal/2,0
K,4,-Lal/2,Wal/2,0
K,5,Lal/2,Wal/2,Hal
K,6,Lal/2,-Wal/2,Hal
K,7,-Lal/2,-Wal/2,Hal
K,8,-Lal/2,Wal/2,Hal
K,9,Lal/2,Wal/2,Hal+Hic
K,10,Lal/2,-Wal/2,Hal+Hic
```

```
K,11,-Lal/2,-Wal/2,Hal+Hic
K,12,-Lal/2,Wal/2,Hal+Hic

V,4,3,2,1,8,7,6,5          !build substate
V,8,7,6,5,12,11,10,9       !build ice
WPOFF,0,0,-0.026           !move work plate
CYL4,d/2,0,0.006,,R/2,,-t  !build PZT disc
CYL4,d/2,0,0,,0.005,,-0.01
WPOFF,0,0,-0.005           !move work plate
CYL4,d/2,0,0.006,,R/2,,-t  !biuld PZT disc
WPOFF,0,0,-0.005           !move work plate
CYL4,d/2,0,0,,R/2,,-0.019  !build steel part
WPOFF,d/2,0,0.01           !move work plate
CONE,R/2,2.25E-2,2.6E-2,0
WPOFF,-d,0,0               !move work plate
WPOFF,d/2,0,2.6E-2         !move work plate
CYL4,d/2,0,0,,0.006,,-0.01
VSBV,ALL,8
VGEN,2,3, , ,-d, , , ,0
VGEN,2,4, , ,-d, , , ,0
VGEN,2,5, , ,-d, , , ,0
VGEN,2,6, , ,-d, , , ,0
VGEN,2,10, , ,-d, , , ,0
VGLUE,ALL          !glue all parts
VSEL,S,VOLU,,2     !select volume 2（ice）and set it with materials 2 &
element 1
VATT,2,,1
VSEL,S,VOLU,,19    !select volume 9（substrate）and set it with materials 1
& element 1
VATT,1,,1
VSEL,S,VOLU,,1
VATT,3,,3          !select volume 1& 3（PZT）and set it with materials 3 &
element 3
VSEL,S,VOLU,,3
VATT,3,,3
VSEL,S,VOLU,,15    !select volume 15& 16（2nd PZT）and set it with
materials 5 & element 3
VATT,5,,3
VSEL,S,VOLU,,16
VATT,5,,3
VSEL,S,VOLU,,13    !select volume 13& 14（steel）and set it with materials
4 & element 1
VATT,4,,1
```

```
VSEL,S,VOLU,,14
VATT,4,,1
VSEL,S,VOLU,,4        !select volume 4&7（bolt）and set it with materials 4 &
element 2
VATT,4,,2
VSEL,S,VOLU,,7
VATT,4,,2
VSEL,S,VOLU,,17       !select volume 17&18（aluminum）and set it with
materials 1 & element 1
VATT,1,,1
VSEL,S,VOLU,,18
VATT,1,,1
VSEL,ALL
ESIZE,0.004,0,  !element size
VSWEEP,1       !mesh
VSWEEP,3
VSWEEP,4
VSWEEP,7
VSWEEP,15
VSWEEP,16

MSHAPE,1,3D
MSHKEY,0
FLST,5,2,6,ORDE,2
FITEM,5,13
FITEM,5,-14
CM,_Y,VOLU
VSEL, , , ,P51X
CM,_Y1,VOLU
CHKMSH,'VOLU'
CMSEL,S,_Y
VMESH,_Y1
CMDELE,_Y
CMDELE,_Y1
CMDELE,_Y2
FLST,5,2,6,ORDE,2
FITEM,5,17
FITEM,5,-18
CM,_Y,VOLU
VSEL, , , ,P51X
CM,_Y1,VOLU
CHKMSH,'VOLU'
CMSEL,S,_Y
```

```
VMESH,_Y1
CMDELE,_Y
CMDELE,_Y1
CMDELE,_Y2
CM,_Y,VOLU
VSEL, , , ,       2
CM,_Y1,VOLU
CHKMSH,'VOLU'
CMSEL,S,_Y
VMESH,_Y1
CMDELE,_Y
CMDELE,_Y1
CMDELE,_Y2
CM,_Y,VOLU
VSEL, , , ,      19
CM,_Y1,VOLU
CHKMSH,'VOLU'
CMSEL,S,_Y
VMESH,_Y1
CMDELE,_Y
CMDELE,_Y1
CMDELE,_Y2
NUMMRG,NODE
```